Please note: Small adjustments to the wording of additions listed in the reviewer response are present in the final manuscript. This was to improve readability. Furthermore, all slight adjustments to results are due to excluding coastal data, as requested by referee D.C.E. Bakker.

Dear Editor,

Below follow comments on the manuscript: “Quantifying the influence of CO_2 seasonality on future ocean acidification” by Sasse et al.

We thank the reviewers for their thorough comments and constructive suggestions. In our response below, we first address comments made by referee M. Hagens, followed by comments made by referee D.C.E Bakker. We hope the manuscript in its revised form will be accepted for publication in Biogeosciences.

Comments and responses to referee M. Hagens.

General comments:

- In my opinion, the manuscript would benefit from exploring changes in future ar seasonality. Previous work has shown that Ω will become more sensitive to changes in CT and AT, as the CT/AT ratio gets closer to unity due to enhanced atmospheric CO2 uptake (Egleston et al, 2010). As a result of this, Ωar seasonality is expected to increase during the 21st century until the point where CT equals AT, which, according to Egleston et al (2010), is reached at high latitudes around 3x the preindustrial pCO2 level (in this context, I could not follow the reasoning on p. 5918, lines 21-23). I understand the difficulties associated with predicting seasonality in carbonate system parameters using ESM and the choice of the authors to use decadal trends in CT and AT from the ESM to predict future Ωar. I would however encourage the authors to add some sensitivity analyses showing the potential effect of a shift in the phase and/or magnitude of CO2 seasonality, especially given that seasonality has been shown to be the dominant mode of contemporary ar variability in the majority of oceanic waters (Fig. 5).
- Response: As a first step to understanding the sensitivity of changes in seasonality we have included the following analysis and paragraph in the manuscript:
  ‘As a first step in assessing the sensitivity of future Ω_{Ar} predictions to shifts in oceanic CO_2 seasonality, we applied a similar approach described above to model output from 6 EMS (Table 2). In this approach, average seasonal cycles in C_T, A_T, temperature and salinity were first computed for the periods 2006 through 2015 and 2091 through 2100. Decadal-mean values from 2091-2100 were then added to the 2006-2015 seasonal cycles, thereby shifting the seasonal cycle to typical values of the years 2090-2100. Finally, seasonal Ω_{Ar} values were computed using both the average 2091-2100 and shifted 2006-2015 C_T, A_T, Temperature and Salinity values. Comparing the seasonal amplitudes in Ω_{Ar} found shifted values were on average 5.4% larger than the

2091-2100 average model output (sd = 48%), with individual model differences ranging from -0.4% to 19.1%. This suggests our data-based Ω_{Ar} amplitudes are on average 5.4% larger than expected if seasonality in C_T, A_T, temperature and salinity was taken into account.'

Understanding how the seasonal phase changes between the two approaches, while very interesting, is beyond the scope of this paper, as the focus of this paper is on the year at which under-saturation occurs, and not the exact month.

Specific comments:

- Manuscript title: the manuscript really focuses on the effects of CO_2 seasonality on Ωar, not other impacts of OA. I would therefore suggest mentioning this more clearly in the title, e.g.: "Quantifying the influence of CO2 seasonality on future aragonite saturation"
- Response: We have changed the title from 'Quantifying the influence of CO_2 seasonality on future ocean acidification' to 'Quantifying the influence of CO_2 seasonality on future aragonite under-saturation onset'

- p. 5911, line 18: given that the CT climatologies represent the nominal year of 2000, why have decadal averages of temperature, salinity and nutrients been used rather than the 1995-2004 years?
- Response: CT climatologies represent the nominal year of 2000 since in-situ measurements collected between 1980 and 2011 were normalised to this year prior to deriving the empirical model by Sasse et al. (2013). By applying the empirical model to the WOA13 decadal averages instead of the 1995-2004 product eliminates the possibility of temporal bias in predicted CT and AT climatologies due to decadal variability in surface temperature, salinity and nutrients. To avoid confusion in the manuscript we have not included this information.

- p. 5912, lines 16-18: I agree that the winter pattern is well captured, with the possible exception of the winter zonal mean around 70S (is this also where the comment on p. 5914, lines 18-21, refers to?), but the summer zonal mean seems to be at the lower edge of the range of measurements around e.g. 60N and 40S. Do you have an explanation for this?
- Response: This likely reflects the combination of spatial and temporal variability skewing the measurements compared to our zonal mean predictions. As referee D.C.E. Bakker correctly comments 'this is not comparing like to like'. To address this issue we have removed the in-situ measurements from figure 2, and added four figures comparing the winter- and summer-time in-situ measurements to the independent predictions in figure 3.

- p. 5915, line 6: it says here that the annual-mean values between 2006 and 2100 are used, but of which emission scenario? Were different results for IAV obtained when another scenario was used?

- Response: We have included details on the emission scenario used to obtain the model-based IAV estimates: 'we de-trended annual-mean projections from 2006 through to 2100 under the RCP8.5 emission scenario'
  We further applied the same analysis to the RCP4.5 and 2.6 emission scenarios. This showed insignificant differences between the three emission scenarios, we have included the following sentence 'These results are independent of the emission scenario used to calculate seasonal and inter-annual variability.'

- p. 5915, lines 26-28: is there a marked difference between the various ESM here? What is the spread in the various model-based relative to data-based seasonal amplitudes? p. 5917, lines 19-26: see general comment above.
- Response: We applied the same analysis to the 6 individual ESM and found similar results. We have included the following sentence in section 5 'We further applied this seasonal amplitude analysis to the 6 individual ESM (table 2) and found amplification factors ranged from 0.8 to 2.3 with a mean and standard deviation of 1.3±0.5.'

- p. 5918, lines 13-18: it is briefly mentioned that by including seasonality the onset of aragonite undersaturation in the Southern Ocean will be brought forward by ca. 8 years relative to the annual mean, while the situation of permanent undersaturation is delayed by ca. 15 years. I think this difference, resulting from the specific seasonal curve of Ωar at this location, is quite interesting and I'm wondering if this non-symmetrical pattern is also observed at other locations. Perhaps the authors could elaborate on this.
- Response: This response is related to the shape of the seasonality curve and will be different in different regions, as shown in the paper. However the goal of paper is not to discuss onset of permanent aragonite under-saturation, rather how its timing is changed by accounting for the seasonality. We've included the following description in the main paper and distribution plot of the year on permanent onset in the supplementary material.
  'Wide-spread onset of permanent Ω_{Ar} under-saturation is only found in the Southern Ocean and Arctic Ocean by the year 2100 (see Fig. S5). In the Southern Ocean, the average time difference between annual-mean and permanent onset is 13.0±5.3 years, which is similar to the time difference between annual-mean and month-long onset at the same locations (13.0±5.9 years). Despite these similar basin-wide values, the correlation coefficient was found to be 0.31, indicating significant spatial differences. This reflects the non-symmetrical nature of seasonal Ω_{Ar} cycles in some regions of the Southern Ocean, as observed in Fig. 6b, which further highlights the importance of accounting for seasonal processes.'

- p. 5918, lines 21-23: see general comment above. With the projected greater sensitivity of Ωar to changes in CT and AT I would expect larger rather than smaller amplitudes. I would be interested in seeing the changes in both the Revelle factor and the amplitude of the Ωar seasonality, as it is not obvious from Fig. 6.

- Response: The discussion of changes in Revelle factor and its implications for future Ω_{Ar} seasonality would require an in-depth discussion that is beyond the scope of the current paper. We have therefore removed the paragraph noting that changes in Ω_{Ar} seasonality is related to shifts in the Revelle factor, as it is not directly relevant to our results.

- p. 5920, lines 5-29: The results of RCP2.6 are presented in Table 2 and Fig. 8 but not discussed at all in this section. I would therefore include a short discussion on this scenario here. p. 5920, lines 27-29: in my opinion this is an interesting conclusion that could be stressed more, e.g. in the abstract.
- Response: We have included the following paragraph in Section 7.2:
  'Under the RCP scenario whereby emissions are drastically reduced in the near future (RCP2.6), our results show very sparse under-saturation onset in the major ocean basins by the year 2100 (Fig. 8). In comparison with projections under RCP8.5, we find a 92.6% (or 83.6×10^6 km^2) reduction in global open-ocean surface waters exposed to at least month-long aragonite under-saturation within the 21st century. Regionally, this reduction increases to 98.9% (62.8×10^6 km^2), 92.8% (9.16×10^6 km^2) and 99.2% (6.8×10^6 km^2) in the Southern Ocean, North Pacific and North Atlantic respectively. This result emphasises the potential difference humanity can make by reducing our CO_2 emissions.'
  We have also included the following sentence in the conclusion:
  'The spatial extent of Ω_{Ar} under-saturation is also drastically reduced under a lower emission scenario. Under RCP2.6 for example, our results show a 92.6% (or 83.6×10^6 km^2) reduction in open-ocean expose to Ω_{Ar} under-saturation compared to projections under RCP8.5, emphasising the importance of mitigating our CO_2 emissions.'

Comments and responses to referee D.C.E. Bakker.

General comments:

Section 2 Methods

- P 5913 L10-11: The text should state CLEARLY that the uncertainties of 10.9 and 9.2 µmol/kg for DIC and TA are for the global ocean south of 70°N and exclude coastal waters (as is stated on page 4332, Figure 12 and Table 6 of Sasse et al., 2013a). The implication is that the results presented in this paper apply only for the global OPEN ocean south of 70°N. The authors might consider blanking areas for which the results are less accurate.
- Response: We have adjusted uncertainty estimates in DIC and TA to represent the global open-ocean region (80N to 80S) and clearly stated this in section 3 'within the global open-ocean'. We have also blanked areas which are less accurate (coastal waters) and excluded data within the coastal region from our analysis. It is important to note these changes did not affect our findings or conclusions due to the small amount of measurements removed.

- P5912. The error analysis of the monthly climatology for omega should be much more thorough.
- Response: We have included two additional error analyses in the main manuscript: 1) we partitioned the global independent Ω_{Ar} residual errors into 14 ocean regions to better evaluate spatial biases within our approach. This includes the addition of a table showing the RSE values for the 14 regions and the following discussion in section 3 'To assess for spatial biases, we partitioned the global independent predictions into 14 regions and calculated RSE values (Table 1; see Fig. S4 for regions). Here we find RSE values lie within ±0.04 units of the global RSE (±0.14) in all regions except the Arctic Ocean, where the RSE value was found to be 0.22. In particular, the Southern Ocean is where our approach excels, predicting Ω_{Ar} values to within ±0.10 units. The small variance of regional RSE values around the global RSE indicates no spatial bias.'
  2) We have included residual standard error plots for summer and winter to assess the models ability to capture seasonal variability, and added the following sentence 'with winter-time and summer-time RSE values of 0.13 and 0.14 respectively (Fig. 3c,e), indicating no strong seasonal bias.'

- P5912. L2. Figure 1 is not very informative. More useful would be a difference plot between in situ measurements and predicted values. Better use might be made of the colour bar if it were to range from 1.0 to e.g. 4.5.
- Response: The purpose of figure 1 is to provide a general feel of our methods ability to capture spatial Ω_{Ar} variability, while section 3 provides an in-depth error analysis. We have therefore decided to not change Figure 1.

- P5912. L13 and Figure 2. The comparison of 'our zonal mean predictions to in situ measurements' is not comparing like with like. It would be instructive to 1) have a comparison of in situ predictions with in situ measurements for winter and summer and 2) zonal mean predictions for winter and summer (Figure 2).
- Response: We have followed this advice and adjusted the figures.

- P5912 L16. The wintertime minimum is clear for the northern hemisphere, but less so for the southern hemisphere.
- Response: This is consistent with our prediction of larger seasonal amplitudes in the northern hemisphere (see Figure 4). We have included the following sentence to comment on this connection: 'The stronger winter-time minimum for the Northern Hemisphere is consistent with our findings or larger seasonal amplitudes in the North Pacific and Atlantic compared to the Southern Ocean (see Fig. 4)'.

Section 3

- L5913. L13. The explanation of the independent predictions is far too short to be understandable. The reader should not have to read another paper to get the basics of this method.
- Response: We have included the following sentence to expand of the independent predictions approach: 'In their approach, measurements from each cruise (N=470) and time-series station (N=2) were individually excluded from the empirical model training phase, and then used as an independent dataset to predict C_T and A_T concentrations. Here, we employ this dataset to calculate…'

- P5913. L23. This analysis does not provide any insight in to spatial biases in the approach, contrary to what the authors state. Extra information on spatial biases (or the absence thereof) would be beneficial.
- Response: We have provided extra information of spatial biases by including a table of regional RSE values and provided the following paragraph 'To assess for spatial biases, we partitioned the global independent predictions into 14 regions and calculated RSE values (Table 1; see Fig. S4 for regions). Here we find RSE values lie within ±0.04 units of the global RSE (±0.14) in all regions except the Arctic Ocean, where the RSE value was found to be 0.22. In particular, the Southern Ocean is where our approach excels, predicting Ω_{Ar} values to within ±0.10 units. The small variance of regional RSE values around the global RSE indicates no spatial bias.'

Conclusions

- The conclusions are a summary of the text. This is not what conclusions should be like. The current conclusions are not very inspiring (as the article was very clear and informative). There is no need for the conclusions to repeat the introduction, nor to describe the methods. The conclusions should not repeat the main text and might be shortened substantially.
- Response: In response to the reviewers comment we have revised the conclusions:

  'Ocean acidification is a global issue which is likely to impact the entire marine ecosystem - from plankton at the base of the food chain to fish at the top. Of particular concern is the decreasing concentration of CO_3^{2-} ions, which lowers the saturation states of $CaCO_3$ minerals (Ω_{Ar} and Ω_{Ca}) and results in detrimental seawater conditions for marine calcifiers (e.g. pteropods and corals; Aze et al., 2014; Fabry et al. 2008) Predicting when critical Ω_{Ar} threshold values will be reached is crucial for projecting the future health of marine ecosystems and for marine resources planning and management. Here we have assessed how seasonality in oceanic CO_2 will influence the future onset of Ω_{Ar} under-saturation.

  The influence of seasonality was evaluated by comparing the difference in future month-long and annual-mean Ω_{Ar} under-saturation onset. Our results suggest seasonality brings forward the initial onset of month-long under-saturation by 17 years

compared to annual mean estimates under RCP8.5, with differences extending up to 35±17 years in the North Pacific due to strong regional seasonality.
Our results also show large-scale under-saturation once atmospheric CO_2 reaches 496ppm in the North Pacific, 517ppm in the North Atlantic and 511ppm in the Southern Ocean, independent of emission scenario. It's important to note that seasonality in these regions was also found to be the dominate mode of variability, accounting for 84±5% of total model-based variability in the Southern Ocean (South of 30°S) and North Pacific (30°N to 70°N). This suggests IAV will not significantly alter onset times found in this study.

Under lower emission scenarios, the average time difference between month-long and annual-mean aragonite under-saturation onset increased from 14 years under RCP8.5 to 32 years under RCP4.5 in the Southern Ocean. This larger time difference under a lower emissions scenario emphasizes the importance of accounting for seasonality when projecting future OA levels under a slower emissions scenario. The spatial extent of Ω_{Ar} under-saturation is also drastically reduced under a lower emission scenario. Under RCP2.6 for example, our results show a 92.6% (or 83.6×10^6 km^2) reduction in open-ocean expose to Ω_{Ar} under-saturation compared to projections under RCP8.5, emphasising the importance of mitigating CO_2 emissions.

Seasonality also influences the spatial pattern of future Ω_{Ar} under-saturation, expanding the latitudinal extent by a global average of 3.5° (or 23×10^6 km^2) towards the equator when compared to annual-mean projections under RCP8.5. From a biogeochemical perspective, this is particularly concerning given the regions of expansion form the poles (~40° to 50° South and North) are known as important hot-spots for $CaCO_3$ export (Sarmiento and Gruber, 2006). Finally, the implication of our results are not limited to the higher latitudes, strong Ω_{Ar} seasonality in some subtropical regions (30°S-30°N; see Fig. 4) will likely bring forward the onset of lower Ω_{Ar} waters by similar temporal periods. Since these regions are rich with sensitive calcifying coral reef ecosystems, considering the influence of seasonality is important when estimating future OA levels and their impacts in these regions.'

Minor comments:

Abstract:

- L5908 L16, L19, L21 Repetition: 'Our results suggest' (3x).
- Response: We have adjusted the abstract to reduce the use to 'Our results suggest'.

Introduction:

- P5908 L25. Consider adding a more recent reference.
- Response: We have updated the reference to the 2015 report.

- P5909. L2. Correct ‘ocean’s’
- Response: This has been corrected.

- P5910. L14. Consider adding a reference to Newton et al. (2014), the GOA-ON report to be found on this page.
- Response: We have included this reference

- P5910 L15-16. It is not clear what the authors want to say: such a large-scale initiative …throughout the global ocean’. Does the 2010 study really comment on the GOAON initiative (which started in or after 2010)?
- Response: We have adjusted the sentence:
  ‘Despite significant efforts over recent years to establish a global carbon measurement network (e.g. the Global Ocean Acidification Observation Network; www.goa-on.org; Newton et al., 2014)), , such a large-scale initiative remains very limited, resulting in only a limited understanding of CO_2 seasonality throughout the global ocean’
  to
  ‘Despite significant efforts over recent years to establish a global carbon measurement network (e.g. the Global Ocean Acidification Observation Network; www.goa-on.org; Newton et al., 2014)), , such a large-scale initiative remains very limited due to spatial and temporal variability in oceanic CO_2 coupled to the high cost of ship time, resulting in only a limited understanding of CO_2 seasonality throughout the global ocean’

- P5911. L5, also P5917 and elsewhere. The authors refer to their TA and DIC climatologies as ‘new global CO2 climatologies’. This is a little confusing.
- Response: We have clarified these sentences by changing ‘the new global climatologies’ to ‘the global climatologies of Sasse et al.’.

Section 2:

- P5911. L12. Correct ‘ocean’s’.
- Response: This has been corrected.

- P5912. L23. Is Popova et al (2014) a ‘data-based’ study? While glancing over it, I could not find much evidence of data being the basis of the (model?) predictions.
- Response: We have modified this sentence to read ‘which is consistent with previous data-based (e.g. Mathis and Questel, 2013) and model-based (e.g. Popova et al., 2014) studies’

Section 3:

- P5913. L21. The figures present a near-normal distribution, not a normal distribution as stated in the text.

- Response: We have adjusted ‘followed a normal distribution’ to ‘followed a near normal distribution’

Section 5:

- P5914. L25. Diurnal variation can play a role in open ocean areas with shallow mixed layers, such as the tropics. There is some older work on this (e.g. Robertson et al., 1993; Bakker et al., 2001; Boutin et al., 1998). Recent studies on surface salinity in a SMOS context are also looking into this (talks at 2014 ESA-SOLAS-EGU conference).
- Response: We have changed ‘Variability in the open-ocean CO_2 system is the combination of seasonal and inter-annual variability’ to ‘Variability in the open-ocean CO_2 system is driven mainly by seasonal and inter-annual variability’. However we maintain that diurnal variability is likely only significant in the coastal domains.

- P5914. L25. Not sure whether (Aze et al. 2014) is the correct way of citing the CBD report. I suspect that the 3 editors played a key role in this report. The report itself provides this citation (page 2): Secretariat of the Convention on Biological Diversity (2014). An Updated Synthesis of the Impacts of Ocean Acidification on Marine Biodiversity (Eds: S. Hennige, J.M. Roberts & P. Williamson). Montreal, Technical Series No. 75, 99 pages.
- Response: This reference has been updated.

- P5915. L8. Did you explain SD?
- Response: We have included a definition of SD (standard deviation).

- P5915. L14. Clarify that this is ‘seasonality is the dominant mode of variability throughout the global ocean in the models’. (add ’in the models’.)
- Response: We have changed ‘This analysis revealed that seasonality is the dominate mode of variability’ to ‘This model-based analysis shows seasonality to be the dominate mode of variability’.

- P5915. L24. ‘consistent’ appears to overstate this pattern. Consider replacing ‘consistent’ by ‘similar’.
- Response: ‘Consistent’ has been replaced with ‘similar’

- P5915. L27. What is the standard deviation (or the range) of the ratio of 1.3?
- Response: We have included the standard deviation (sd = 0.5).

- P5916. L1. Add ‘This suggests ESM on average under-predict’.
- Response: We have added ‘on average’.

Section 6:

- P5916. L13. The authors casually state that surface ocean pCO2 would track the increase in atmospheric CO2. What is this statement based on? Clarify which implicit assumptions this statement relies on. Add a reference.

  Response: We have added 'regionally integrated' and 'over longer timescales' into the following sentence to clarify: 'the rate of increase in regionally integrated ocean surface pCO_2 would have roughly tracked the atmospheric CO_2 growth rate over longer timescales'. We have also included the reference (Lenton et al., 2012; Tjiputra et al., 2014).
- P5916. L13-14. The authors state that this was 'likely adequate for most of the 20th century'. What do the authors mean with 'likely adequate'? What do the authors base this statement on? Is this a model result? If so, say so. Only in recent decades is data coverage of ocean carbon parameters sufficiently large for trend analysis of surface ocean CO2 (e.g. Takahashi et al., 2009).
- Response: We have omitted the sentence 'Although this was likely adequate for most of the 20th century'. This sentence is not necessary and confuses the message.

- P5917. L2. The authors mention an increase in the CO2 disequilibrium. What is this based on? A reference would be appropriate.
- Response: We have included 'described above' to clarify what this is based on, and added the reference (McNeil and Matear, 2013).

Section 7:

- P5918. L8. Why are these sites 'unique'? Consider removing the word 'unique'. Presumably you mean that these are 'single' sites, but that these sites are somewhat representative for the wider region.
- Response: We have changed 'unique' to '1°x1°' and included 'which are somewhat representative of the larger region'

- P5918. L21-23. The statement on a reduction in seasonal amplitudes of omega as a result of changes in the Revelle factor needs better explanation and possibly a reference to earlier studies observing something similar. The current text is rather cryptic.
- Response: The discussion of changes in Revelle factor and its implications for future Ω_{Ar} seasonality would require an in-depth discussion that is beyond the scope of the current paper. We have therefore removed the paragraph noting that changes in Ω_{Ar} seasonality is due to shifts in the Revelle factor, as it is not directly relevant to our results.

- P5919. L3-4 and L11. Add 'the year', in 'by the year 2086' and 'as early as the year 2030'.
- Response: These have been added

- P5919. L5. Correct ‘century’s’. (??)
- Response: We have change ‘centuries end’ to ‘the year 2100’

- P5920. L2. Remove ‘before this occurs’ as this overlaps with ‘before’ later in the sentence.
- Response: This sentence has been adjusted accordingly.

- P5920. L21. Add ‘the’ in ‘the Southern Ocean’.
- Response: ‘the’ has been added.

Section 8:

- Section 8. P5921. L8. Do you mean ~3.5° latitude’? Clarify.
- Response: we have changed ‘increases by ~3.5°’ to ‘shifted equatorward by ~3.5° degrees’

- P5921 L10. Remove ‘additional’. This is not really additional.
- Response: ‘an additional’ has been removed.

- P5921. L13. ‘Much earlier than anticipated’. What is this based on? Clarify.
- Response: We have included ‘under previous annual-mean projections (e.g. Orr et al. 2005).’ To clarify.

Conclusions:

- P5921 L20. Remove or clarify ‘at the base’ and ‘at the top’.
- Response: We have included ‘of the food chain’ to clarify.

- P5921 L21-L22. Saturation states and minerals are plural, however, you only provide the symbol for omega aragonite. Correct.
- Response: ‘and Ω_{Ca}’ was added.

Quantifying the influence of CO_2 seasonality on future aragonite under-saturation onset ~~ocean acidification~~

T. P. Sasse[1], B. I. McNeil[1], R. J. Matear[2] and A. Lenton[2]

[1] {Climate Change Research Centre, Kensington Campus, University of New South Wales, Sydney, Australia}

[2] {CSIRO Oceans and Atmosphere National Research Flagship, Hobart, Australia}

Correspondence to: T. P. Sasse (t.sasse@unsw.edu.au)

Abstract

Ocean acidification is a predictable consequence of rising atmospheric carbon dioxide (CO_2), and is highly likely to impact the entire marine ecosystem - from plankton at the base of the food chain to fish at the top. Factors which are expected to be impacted include reproductive health, organism growth and species composition and distribution. Predicting when critical threshold values will be reached is crucial for projecting the future health of marine ecosystems and for marine resources planning and management. The impacts of ocean acidification will be first felt at the seasonal scale, however our understanding how seasonal variability will influence rates of future ocean acidification remains poorly constrained due to current model and data limitations. To address this issue, we first quantified the seasonal cycle of aragonite saturation state utilizing new data-based estimates of global ocean surface dissolved inorganic carbon and alkalinity. This seasonality was then combined with earth system model projections under different emissions scenarios (RCPs 2.6, 4.5 and 8.5) to provide new insights into future aragonite under-saturation onset. Under a high emissions scenario (RCP 8.5), our results suggest accounting for seasonality will bring forward the initial onset of month-long under-saturation by 17±10 years compared to annual-mean estimates, with differences extending up to 35±16 ~~17~~ years in the North Pacific due to strong regional seasonality. ~~Our results also show~~ This earlier onset will result in large-scale under-saturation once atmospheric CO_2 reaches ~~486~~ 496ppm in the North Pacific and 511ppm in the Southern Ocean, independent of emission scenario. ~~Our results~~ This work suggests ~~that~~ accounting for seasonality is critical to projecting the future impacts of ocean acidification on the marine environment.

1. Introduction

The global ocean currently absorbs about 30% of annual fossil-fuel CO_2 emissions (Le Quéré et al., 2015), and will likely sequester up to 80% of all human-derived CO_2 emissions over the coming centuries (Archer et al., 1997). While this ecosystem service largely mediates the rate of climate change, the immediate impact of this additional CO_2 is a shift in the ocean's chemical composition, resulting in lower pH and carbonate ion (CO_3^{2-}) concentrations - commonly referred to as ocean acidification (OA; Caldeira and Wickett, 2003).

Of great concern to marine ecosystems is the immediate impact OA is presenting to multiple ~~marine~~ organisms. This includes organisms that require an adequate supply of CO_3^{2-} to form and preserve their calcium carbonate ($CaCO_3$) shells and skeletons (e.g. corals, pteropods and coccolithophorids). Two key parameters for understanding how a change in CO_3^{2-} impacts marine calcifiers are the saturation states for aragonite (Ω_{Ar}; Eq. 1) and calcite (Ω_{Ca}; Eq. 2) - the two main $CaCO_3$ minerals formed by marine calcifiers.

$$\Omega_{Ar} = [Ca^{2+}][CO_3^{2-}]/K^*_{sp(Ar)} \quad (1)$$

$$\Omega_{Ca} = [Ca^{2+}][CO_3^{2-}]/K^*_{sp(Ca)} \quad (2)$$

Here, $[Ca^{2+}]$ and $[CO_3^{2-}]$ represent the concentrations of calcium and carbonate ions respectively, while $K^*_{sp(Ar)}$ and $K^*_{sp(Ca)}$ are the apparent stoichiometric solubility products for aragonite and calcite. Laboratory and mesocosm experiments suggest production and dissolution of biogenic $CaCO_3$ are mainly controlled by seawater Ω levels (Aze et al., 2014; Fabry et al., 2008). These experiments further indicate significant decreases in calcification rates when test species are exposed to Ω levels below their natural range for periods of days to weeks (Chan and Connolly, 2013). Once seawater Ω levels fall below 1, referred to as under-saturation, seawater becomes corrosive to $CaCO_3$ and dissolution can occur. Although experimental studies show detrimental impacts at seawater Ω levels above 1 (e.g., Bednarsek et al., 2012; Fabry et al., 2008), under-saturation is widely regarded as a key threshold value (e.g., Hunt et al., 2008; Orr et al., 2005). Since aragonite is approximately ~~about~~ 50% more soluble than calcite, resulting in earlier under-saturation, ~~we~~ the focus of this work is on future changes in Ω_{Ar}.

Several previous studies have used Earth System Models (ESM) to predict future annual-mean Ω_{Ar} levels under different CO_2 emission scenarios (Caldeira and Wickett, 2003, 2005; Cao et al., 2007; Kleypas et al., 1999; Orr et al., 2005; Ricke et al., 2013). These annual-mean projections suggest under-saturation will occur in the Southern Ocean and high northern latitudes within the 21st century (e.g. Orr et al., 2005). However, strong natural seasonality in oceanic CO_2 ~~within these regions~~ has the potential to significantly alter the onset of future under-saturation, not captured by these approaches.

McNeil and Matear (2008) first demonstrated how strong CO_2 seasonality in the Southern Ocean brings forward the initial onset of month-long aragonite under-saturation conditions by ~30 years relative to annual-mean projections. More recent studies in Australia's Great Barrier Reef (Shaw et al., 2013), Californian coast (Gruber et al., 2012) and Arctic Ocean (Steinacher et al., 2009) further demonstrate the importance of accounting for natural CO_2 seasonality when evaluating future OA levels.

Despite significant efforts over recent years to establish a global carbon measurement network (e.g. the Global Ocean Acidification Observation Network; www.goa-on.org; (Newton et al., 2014)), such a large-scale initiative remains very limited by spatial and temporal variability in oceanic CO_2 coupled to the high cost of ship time, resulting in only a limited understanding of CO_2 seasonality throughout the global ocean (Monteiro et al., 2010). This represents a critical gap in our ability to understand and predict the influence of natural variability for the future onset and duration of critical OA levels.

It is important to note that ESMs do provide some insights into regional CO_2 seasonality. However, it has been shown the current generation of ESMs do not accurately capture the observation-based magnitude and/or phase of air-sea CO_2 fluxes in most ocean regions, including the Southern Ocean, North Pacific, Indian Ocean and North Subpolar Atlantic (Ishii et al., 2014; Lenton et al., 2013; Pilcher et al., 2015; Sarma et al., 2013; Schuster et al., 2009). Consequently, these models do not realistically characterize the seasonality of Ω_{Ar}.

Here, we use newly constrained data-based estimates of global ocean surface dissolved inorganic carbon (C_T) and alkalinity (A_T) of Sasse et al. (2013b) to diagnose monthly Ω_{Ar} distributions for the nominal year of 2000. We then project our monthly observational baselines through to 2100 using decadal trends from an ensemble of Earth System climate models (CMIP5) forced under different emissions scenarios (RCPs 2.6, 4.5 and 8.5). These results provide new insights into the influence of sea-surface seasonality on the likely onset times for future aragonite under-saturation in the global ocean.

The work presented here expands on the study of McNeil and Matear (2008) with several key improvements: 1) the ~~new~~ global CO_2 climatologies of Sasse et al. (2013b) better reflect the latest observations and were derived using a more sophisticated method; 2) we explore the potential for CO_2 disequilibrium to evolve into the future by exploiting CMIP5 model projections; 3) we project our observational baseline using three different emission scenarios (RCP2.5, 4.5 and 8.5); 4) we apply the approach globally rather than the Southern Ocean alone.

2. Diagnosing monthly carbon system distributions

The ocean's inorganic carbon system can be fully constrained by knowing any two parameters within its inorganic carbon constituents - partial pressure of CO_2 (pCO_2), dissolved inorganic carbon (C_T), total alkalinity (A_T) or pH (Dickson et al., 2007). Here we diagnose monthly Ω_{Ar} distributions using ~~the newly constrained monthly~~ the 1°×1° C_T and A_T monthly climatologies of Sasse et al. (2013b) in combination with the World Ocean Atlas 2013 (WOA13) temperature, salinity, and nutrient monthly surface distributions (Objectively analysed decadal averages; Garcia et al., 2014a, b; Locarnini et al., 2013; Zweng et al., 2013). Since the C_T climatologies of Sasse et al. (2013b) were predicted for the nominal year of 2000 (see Sasse et al. (2013b) for details), the ~~our~~ Ω_{Ar} values calculated here are also representative of this year.

All calculations were conducted using the total pH scale and carbonic acid dissociation constants of Mehrbach et al (1973) as refitted by Dickson and Millero (1987), K_{SO_4} dissociation constant of Dickson (1990b) and boric acid dissociation constant of Dickson (1990a). Calculations of Ω_{Ar} used the K_{sp} values of Mucci (1983) and [Ca]-salinity relationship of Riley and Tongudai (1967).

To evaluate the realism of our global Ω_{Ar} predictions, we compare the network of in-situ Ω_{Ar} values to our corresponding 1°×1° predictions for the same month and location (Fig. 1). In-situ Ω_{Ar} values were calculated using measured A_T and C_T concentrations, where C_T values were first normalised to the year 2000 via observed Revelle factors and assuming constant equilibrium with the atmospheric CO_2 increase (see Sasse et al. (2013b) for details). Our data-based approach is consistent with the general pattern of high Ω_{Ar} values in the tropics which decrease poleward. Our approach also captures well the strong Ω_{Ar} gradients at ~40° North and South and local Ω_{Ar} minimas in equatorial upwelling regions (see Fig. S1 in the Supplement for monthly Ω_{Ar} distributions). Statistical analysis finds the ~~root mean square difference (RMSD) and~~ correlation between the global in-situ values and our corresponding space/month 1°×1° predictions to be ~~0.17 and~~ 0.98 ~~respectively~~.

We further compare our zonal mean 1°×1° Ω_{Ar} predictions for summer and winter to ~~the in-situ measurements to~~ evaluate the ability of our approach to capture seasonal variability (Fig. 2). ~~Our data-based reconstruction~~ The data-based zonal pattern compares well to the general understanding of ~~zonal pattern, showing~~ a strong winter-time minimum in the higher latitudes ~~. This winter-time signal is~~ driven by ~~the combination of~~ surface cooling and strong persistent winds that ventilate deep-waters depleted in CO_3^{2-} (McNeil and Matear, 2008). The stronger winter-time minimum in the Northern Hemisphere is consistent with our findings of larger seasonal amplitudes in the North Pacific and North Atlantic compared to the Southern Ocean (see Fig. 4).

Our monthly data-based Ω_{Ar} distribution also reconfirms ~~that~~ the contemporary ocean surface is supersaturated with respect to aragonite, showing 99.3% of monthly ocean surface waters with Ω_{Ar} levels greater than 1 in the year 2000. The only region where month-long under-saturation was found is in the Arctic Ocean (see Fig. S2), which is consistent with previous data-based (e.g. Mathis and Questel, 2013) and model-based (e.g. Popova et al., 2014) studies.

An independent data-based climatology for monthly ocean surface Ω_{Ar} was presented by Takahashi et al (2014; hereinafter referred to as T14). In their approach, global Ω_{Ar} distributions were calculated for the nominal year of 2005 on a 4°×5° resolution using a combination of interpolated ocean-surface $p\mathrm{CO}_2$ and predicted A_T values via a salinity and nitrate relationship. Estimates in the equatorial Pacific were however omitted due to strong inter-annual variability.

Comparison between T14 and our global Ω_{Ar} values (projected to the year 2005; see Sect. 6) reveals a global correlation of 0.99, with mean Ω_{Ar} values of 2.68 and 2.72 respectively. This good agreement between two independent data-based approaches provides additional confidence in our estimated Ω_{Ar} values. Several key benefits in using our Ω_{Ar} baseline include: 1) better spatial resolution; 2) inclusion of the equatorial Pacific; 3) independent uncertainty estimates in our Ω_{Ar} predictions.

3. Quantifying uncertainties in our Ω_{Ar} predictions

The approach used here to diagnose surface Ω_{Ar} distributions includes both systematic and random sources of error. The main source of random error derives from uncertainties within the global open-ocean C_T and A_T distributions, which have been estimated to be ±11.8 ~~10.9~~ and ±10.2 ~~9.2~~ μmol kg^{-1} respectively (Sasse et al., 2013b). To quantify the corresponding uncertainty in our calculated Ω_{Ar} values, we applied an independent testing approach using 16,727 mixed-layer C_T and A_T independent predictions of Sasse et al (2013b). In their ~~this~~ approach, measurements from each cruise (N=470) and time-series station (N=2) were individually excluded from the empirical model training phase, and then used as an independent dataset to predict C_T and A_T concentrations. Here we employed this dataset to calculated Ω_{Ar} values using both the in-situ C_T and A_T measurements and their corresponding independent predictions. Comparison between these values revealed a global uncertainty in our Ω_{Ar} predictions to be ±0.138 (Residual Standard Error (RSE); Fig. 3a), with summer-time and winter-time RSE values of 0.142 and 0.126 respectively (Fig. 3c,e), indicating no strong seasonal biases.

To evaluate our approach for systematic errors, we analysed the global distribution of residual errors via the independent testing approach described above (Fig. 3b). We further partitioned the residuals by season to evaluate for any temporal bias (see Fig. 3d,f). The global, summer-time and winter-time residual error distributions all followed a near normal distribution with mean residual errors of 0.004, 0.001 and 0.007, respectively. This suggests no strong ~~spatial or~~ global or temporal biases exist in our approach.

To assess for spatial biases, we partitioned the global independent predictions into 14 ocean regions and calculated RSE values (Table 1; see Fig. S3 for regions). Here we find all regional RSE values lie within ±0.04 units of the global RSE (0.138), with the exception the Arctic Ocean, where the RSE value was 0.22 (N=673). In particular, the Southern Ocean is where our approach excels, predicting Ω_{Ar} values to within ±0.10 units (N=2923). The small variance in regional RSE values around the global value indicates no spatial bias.

Finally, it is important to acknowledge that uncertainties and biases in the WOA13 objectively analysed products will influence our data-derived Ω_{Ar} distributions. Since error estimates in the WAO13 products remain uncertain, this source of uncertainty cannot be accounted for at this time. However, if we assume errors in WOA13 are uncorrelated and much smaller than errors associated with the carbonate system, then they will not significantly contribute to uncertainty in our calculated Ω_{Ar} values.

4. How large is contemporary seasonal variability?

Seasonal amplitudes were calculated here as the difference between the maximum and minimum monthly Ω_{Ar} values in each 1°×1° grid cell (Fig. 4). From a global open-ocean perspective, seasonality was found to be 0.46±0.25 (1σ), while strong regional mixing/upwelling regimes and/or biological production results in large spatial differences. In the high Northern latitudes (45°N to 70°N) and Southern subtropics (20°S to 45°S) for example, seasonality was found to be strongest at 0.73±0.20 and 0.46±0.14 (1σ) respectively, while seasonality in the equatorial region (20°N to 20°S) was found to be weakest at 0.34±0.21.

From an OA perspective, regions where seasonality is strongest will have the largest implications for the future onset of critical Ω_{Ar} levels. In the tropics for example, where aragonite secreting corals are abundant (Tupper et al., 2011), the relatively weak seasonality will result in little difference between month-long and annual-mean onset for future Ω_{Ar} levels. In the higher latitudes however, where seasonality is largest, the implications for future Ω_{Ar} onset will be much more pronounced.

It must be noted that our seasonal predictions will underestimate some coastal regions where limited data exists. Along the coastal Antarctic continent for example, in-situ data has shown seasonal Ω_{Ar} variability of up to 1.75 (McNeil et al., 2010), which is not captured by our approach.

5. Is seasonality the dominant mode of Ω_{Ar} variability?

Variability in the open-ocean CO_2 system is driven mainly by ~~the combination of~~ seasonal and inter-annual variability (IAV), with diurnal variability only playing a significant role in coastal waters (Secretariat of the Convention on Biological Diversity., 2014).

To quantify the relative roles of seasonal and IAV in open-ocean waters, we analysed results from an ensemble of 6 ESM participating in the Coupled Model Inter-comparison 5 project (CMIP5; Table 2). Each model was first re-gridded to a 1°×1° resolution ~~via a binominal~~

~~interpolation,~~ and Ω_{Ar} values calculated via the standard CO_2 dissociation constants described in Sect. 2. To constrain the total magnitude of natural variability, we combined the seasonal and IAV signals within each 1°×1° grid cell (Fig. 5a). For IAV, we de-trended annual-mean projections from ~~values between~~ 2006 through to~~and~~ 2100 under the RCP8.5 emission scenario via a third order polynomial, and then calculated the standard deviation (SD) in the de-trended data (i.e. 95.4% of the year-to-year variance). For seasonality, we used the average seasonal magnitude (maximum minus minimum) between 2006 and 2016. The relative roles of variability were finally quantified by dividing the individual components by the total variability. We also multiplied these values by 100 to present the relative roles of seasonal variability and IAV as a percentage of the total natural variability (Figs. 5b,c).

This model-based analysis revealed ~~that~~ seasonality ~~is~~ to be the dominant mode of variability throughout the global open-ocean, accounting for 74±12% (1σ) of total natural variability. From a regional perspective, seasonality is the dominant mode in the higher latitudes, accounting for 84±5% of total variability in the Southern Ocean (South of 30°S) and North Pacific (30°N to 70°N). In the eastern equatorial Pacific however, IAV is the dominant mode of variability, representing up to 70% of total variability (Fig. 5c). With the exception of the central equatorial Pacific, seasonality is the dominant mode of variable across the greater equatorial region (30°S to 30°N), accounting for 67±12% of the total natural variability within this region (Fig. 5b). These results are independent of the emission scenario used to calculate the seasonal and inter-annual variability components.

Comparison between our data-based Ω_{Ar} seasonal amplitudes (Fig. 4) and model-based total variability (Fig. 5a), reveals a ~~consistent~~ similar spatial pattern in regions where seasonality is the dominant mode (i.e. North Pacific, Southern Ocean and West North Atlantic). Despite this general agreement, we find ~~that~~ our data-based seasonal estimates are on average 1.3 times larger than the 2006-2016 model-based mean seasonal amplitudes in the North Atlantic, North Pacific and Southern Ocean (SD=0.5; see Fig. S4). We further compared our databased seasonal amplitudes for the year 2000 to the 2006-2016 mean seasonal amplitudes predicted by the 6 individual ESM (Table 2). Here we found amplification factors for our seasonal Ω_{Ar} amplitudes ranged from 0.8 to 2.3, with a mean and standard deviation of 1.3±0.5. This suggests ESMs~~s~~ on average under-predict the oceans seasonal CO_2 cycle by a factor of 1.3 (or 30%) ~~and therefore its role in driving the total natural variability~~.

6. Projecting future Ω_{Ar} levels

Exchange of CO_2 between the ocean and atmosphere is driven by the air-sea gradient in *p*CO_2. Each year, approximately 70 petagrams of carbon is naturally exchanged at the air-sea interface in both directions (Sarmiento and Gruber, 2002). Comparison between ocean-surface and atmospheric *p*CO_2 reveals seasonality in the ocean is the dominant driver of this large natural CO_2 flux (Sasse et al., 2013a; Takahashi et al., 2009), which in turn is driven by biological and physical-solubility processes (Sarmiento and Gruber, 2006) - referred to here as the natural cycling of carbon.

If the natural cycling of carbon remained in steady-state throughout the last two centuries, the rate of increase in regionally integrated ocean surface *p*CO_2 would have roughly tracked the atmospheric CO_2 growth rate over longer timescales (Lenton et al., 2012; Tjiputra et al., 2014).~~ Although this was likely adequate for most of the 20th century, r~~Recent studies have however identified shifts in the oceans natural cycling of carbon due to climate related alterations. For example, decadal-scale trends in ocean surface temperature (Levitus et al., 2005; Lyman et al., 2010) and salinity (Durack and Wijffels, 2010) are influencing both the solubility of CO_2 and ocean circulation pathways, while shifting wind patterns are impacting circulation and seasonal mixing processes, resulting in either enhanced or diminished ventilation of deep waters enriched with C_T and nutrients (e.g. Le Quéré et al., 2007; Lenton et al., 2009).

Added to this climate-mediated change in oceanic CO_2 uptake, the air-sea exchange of CO_2 is a slow process (approximately 1 year equilibration time), where local physical and biological processes can cause the ocean to deviate from atmospheric CO_2. This creates a difference between the atmospheric and ocean surface *p*CO_2 (disequilibrium). Further, as atmospheric CO_2 increases, ocean processes can cause the ocean to lag the atmospheric increase and the disequilibrium term to increase with time (McNeil and Matear, 2013). For example, in the polar regions, short residence times of surface waters and the ventilation of old CO_2-rich deep waters creates an increasing CO_2 disequilibrium, resulting in a growing difference between atmospheric and surface ocean CO_2 over time.

To account for the effects of future climate change and increasing CO_2 disequilibrium described above, we projected our data-based CO_2 climatologies using results from an ensemble of 6 ESM (Table 2). In this approach, decadal trends in C_T, A_T, temperature and salinity were combined with our monthly data-based C_T and A_T and WOA13 temperature and salinity products. Monthly Ω_{Ar} values were then calculated using the standard CO_2 dissociation constants presented in Sect. 2.

We projected our CO_2 base-lines using ESM results forced under several different Representative Concentration Pathways (RCP8.5, 4.5 and 2.6). Here, RCP8.5 is a *business-as-usual* scenario with little mitigation and peak CO_2 concentrations at 935 parts per million (ppm) in the year 2100; RCP4.5 is a scenario where emissions peak in mid-century and are then slowly reduced, resulting in a peak CO_2 concentration of 538ppm by 2100; finally, RCP2.6 is a *best-case* scenario were emissions are dramatically reduced in the near future to the point where more CO_2 is absorbed by the ocean and terrestrial biosphere than emitted by human activities (Meinshausen et al., 2011).

It should be emphasised that the observation-based CO_2 climatologies of Sasse et al (2013b) have been shown to accurately reconstruct the global pattern of present-day ocean surface CO_2 variability. However, for this study we assume constant seasonality from our baseline CO_2 climatologies throughout the 21st century. Although this assumption is likely adequate for short temporal projections (<10years), a recent evaluation of 10 ESM suggests large changes in mixing, biological production and CO_2 solubility will occur within the 21st century (Bopp et al., 2013). By projecting our base-line climatologies using decadal trends from ESM we implicitly capture the decadal response to these changes, however, any potential shift in the phase and magnitude of CO_2 seasonality are not explored in our approach.

Given the limitations in the current generation of ESM in capturing seasonality in air-sea CO_2 flux and/or ocean surface pCO_2 in many important regions (Ishii et al., 2014; Lenton et al., 2013; Pilcher et al., 2015; Sarma et al., 2013; Schuster et al., 2009), their ability to realistically project future changes in CO_2 seasonality is questionable. We therefore do not account for any change in CO_2 seasonality in the current study. Once models evolve to a point where seasonality of the carbon system is well-represented, potential future changes to seasonality will need to be explored in future studies.

As a first step to assessing the sensitivity of future Ω_{Ar} predictions to shifts in oceanic CO_2 seasonality, we applied the following approach to model output from 6 ESM (Table 2). Seasonal cycles in C_T, A_T, temperature and salinity were first averaged over the decades 2006 through 2015 and 2091 through 2100 in each 1°×1° grid cell. Decadal-mean values from the 2091-2100 period were then added to the 2006-2015 mean seasonal cycles, thereby shifting the earlier seasonal cycle to typical values of the years 2090-2100. Finally, seasonal Ω_{Ar}

values were computed using both the mean 2091-2100 and shifted 2006-2015 seasonal C_T, A_T, Temperature and Salinity values. Comparing the seasonal amplitudes in Ω_{Ar} found shifted values were on average 5.4% larger than the 2091-2100 period for the global open-ocean (SD=48%), with individual model differences ranging from -0.4% to 19.1%. This suggests our data-based Ω_{Ar} amplitudes are on average 5.4% larger than expected if changes in C_T, A_T, temperature and salinity seasonality were taken into account.

7. Quantifying the onset of aragonite under-saturation

When strong natural carbon seasonality is combined with a long-term trend, the onset and exposure times of biological thresholds are influenced. To illustrate this point, we present Ω_{Ar} projections under the *business-as-usual* scenario (RCP8.5) at two 1°x1°~~unique~~ sites in the North Atlantic and Southern Ocean which are somewhat representative of the larger region (Fig. 6). At the North Atlantic site, strong seasonality was found to bring forward the initial onset (time a in Fig. 6a) of aragonite under-saturation by 27 years relative to the annual-mean (time b; Fig. 6a), while weaker variability at the Southern Ocean site brings forward under-saturation by 8 years (Fig. 6b). It's important to emphasize that monthly under-saturation conditions starts at time a, and then eventually extends to be permanent over all months (time c). As much as seasonality brings forward the initial onset of under-saturation, it also delays the permanent onset (Fig. 6). At the Southern Ocean site for example, seasonality delays the permanent onset by ~15 years. In the context of ocean acidification impacts, monthly exposure times are important, since laboratory experiments show that even short exposure times (i.e. hours to days) can result in significant implications to the health and well-being of the test species (Chan and Connolly, 2013).

~~Note that our reconstructed seasonal amplitudes were initially constant, however as ocean carbon chemistry changed with additional CO_2 input (i.e. changes in the Revelle factor), the amplitudes of the calculated Ω_{Ar} reduced.~~

7.1 Future Ω_{Ar} levels under RCP8.5

Under the *business-as-usual* scenario (RCP8.5), our results show annual-mean aragonite under-saturation will occur by the year 2086±9 (1σ) in the North Pacific and North Atlantic, 2074±12 in the Southern Ocean, while tropical and temperate regions (~40°S to ~40°N) will remain super-saturated beyond the year 2100 ~~centuries end~~ (Fig. 7a). When seasonality is considered, the initial month-long onset precedes annual-mean estimates by a global average of 17±10 years (1σ) under the RCP8.5 scenario (70°N to 70°S; Figs. 7b-c). In the North Pacific and North Atlantic, where seasonality is strongest, month-long under-saturation is brought forward by ~~38±18~~ 36±16 and ~~20±7~~ 19±6 years respectively (Fig. 7c).

In the Southern Ocean (South of 60°S), our results show month-long aragonite under-saturation will first occur as early as the year 2030, or when atmospheric CO_2 concentrations reach ~450ppm. While this is consistent with projections by McNeil and Matear (2008) under the IPCC IS92a scenario, our results show seasonality will delay the onset of annual-mean under-saturation by 14±7 years, which is half the delay time found by McNeil and Matear (2008). This difference likely reflects the faster rate of change in atmospheric CO_2 under RCP8.5 compared to IPCC IS92a, while differences in seasonality found by the two approaches is likely a secondary factor.

Wide-spread onset of permanent Ω_{Ar} under-saturation is only found in the Southern Ocean and Arctic Ocean by the year 2100 (see Fig. S5). In the Southern Ocean, the average time difference between annual-mean and permanent onset is 13.0±5.3 years, which is similar to the time difference found between annual-mean and month-long onset at the same locations (13.0±5.9 years). Despite these similar basin-wide time difference values, the correlation coefficient was found to be 0.31, indicating significant spatial differences. This reflects the non-symmetrical nature of seasonal Ω_{Ar} cycles in some regions of the Southern Ocean, as observed in Fig. 6b, which further highlights the importance of accounting for seasonal processes.

Early aragonite under-saturation is of particular concern for the many important calcifying organisms that inhabit the higher latitudes. Pteropods for example, are a zooplankton species that forms aragonite shells to provide ballast for vertical migration in search of food and breeding. In the Southern Ocean, pteropods have been found to represent up to 30% of total zooplankton (Hunt et al., 2008), and are themselves important prey for larger zooplankton, as well as many fish and bird species (Hunt et al., 2008; Karnovsky et al., 2008). From a biogeochemical perspective, pteropods account for at least 12% of the global $CaCO_3$ flux into the ocean interior (Berner and Honjo, 1981). When pteropods sink to depths at which $\Omega_{Ar} = 1$, known as the saturation horizon or lysocline, field studies show significant dissolution occurs (Hunt et al., 2008). As more anthropogenic CO_2 enters the ocean system, the aragonite saturation horizon will approach the upper ocean until the surface waters become permanently under-saturated. Decade(s) b~~B~~efore this occurs however, seasonality ~~variability~~ will expose calcifying organisms to month-long under-saturation conditions, causing unknown changes to the health of the wider marine ecosystem ~~decade(s) before the annual mean value becomes under-saturated~~.

7.2 Future Ω_{Ar} levels under RCP 4.5 and 2.6

In the previous section we presented results under the RCP8.5 scenario. We now explore how lower emission scenarios influence future onset of aragonite under-saturation. We consider our Ω_{Ar} projections under RCP4.5, 2.6 and their behaviour relative to RCP8.5 (Table 3 and Fig. 8). In the North Pacific, we find month-long aragonite under-saturation occurs by the year 2057±24 ~~2052±27~~ and 2040±15 ~~2037±18~~ under RCP4.5 and 8.5, respectively. Despite this difference in onset year, atmospheric CO_2 concentrations at time of onset are consistent at 492±45ppm ~~481±54ppm~~ and 501±60 ~~491±69ppm~~ for RCP4.5 and 8.5 respectively, with a correlation co-efficient of 0.75 ~~82~~ (Table 3). As expected, this suggests under-saturation onset is highly dependent on the atmospheric CO_2 concentration, where we find large scale under-saturation in the North Pacific once atmospheric CO_2 reaches 496ppm ~~486ppm~~ (mean of RCP4.5 and 8.5). Similarly, our results suggest wide spread aragonite under-saturation will occur when atmospheric CO_2 reaches concentrations of 517ppm ~~506ppm~~ in the North Atlantic and 511ppm in the Southern Ocean.

Under RCP2.6, whereby emissions are drastically reduced in the near future, our results show very sparse under-saturation onset in the major ocean basins by the year 2100 (Fig. 8). When compared to projections under RCP8.5, we find a 92.6% (or 83.6×10^6 km^2) reduction in global open-ocean surface waters exposed to at least month-long aragonite under-saturation within the 21st century. Regionally, this reduction increases to 98.9% (62.8×10^6 km^2), 92.8% (9.16×10^6 km^2) and 99.2% (6.8×10^6 km^2) in the Southern Ocean, North Pacific and North Atlantic respectively. This result highlights the potential difference humanity can make by reducing CO_2 emissions in the near future.

To further probe the influence of a lower emission scenario on future OA onset, we compare the time difference between month-long and annual-mean aragonite under-saturation onset under RCP8.5 and RCP4.5 at 457 ~~468~~ 1°×1° grid cell locations in the Southern Ocean (Figs. 8a and 7b). Here we find the average onset for month-long under-saturation occurs by the year 2048 under RCP8.5, and 2073 under RCP4.5. Despite the lower emission scenario delaying the initial onset, we find that the time difference between month-long and annual mean onset is 18 years longer under RCP4.5 compared to RCP8.5 (i.e. 14 years under

RCP8.5 and 32 years under RCP4.5). This longer time delay under RCP4.5 emphasizes that seasonality becomes even more important when projecting future OA levels under a slower emissions scenario.

8 How does seasonality influence the geographical extent of aragonite under-saturation?

Accounting for seasonality also presents significant implications for the spatial pattern of future aragonite under-saturation~~ by the end of the 21st century~~. Here we refer to regions where seasonality induces at least month-long under-saturation conditions while annual-mean Ω_{Ar} projections remain super-saturated throughout the 21st century. By the year 2100, the latitudinal extent of ocean surface exposed to at least month-long aragonite under-saturation will have ~~increased~~ shifted equatorward by ~3.5° degrees relative to the extent of annual-mean estimates under the RCP8.5 scenario (Fig. 9). This extension translates to ~~an additional ~25×10^6^~~ ~23×10^6 km^2 of open-ocean surface (or ~~7.2%~~ 6.8% of total open-ocean area) exposed to at least month-long aragonite under-saturation by 2100 under the *business-as-usual* scenario (RCP8.5). This expansion of corrosive aragonite conditions is likely to impact multiple marine calcifiers living within these regions much earlier than anticipated under previous annual-mean projections (e.g. Orr et al., 2005). Pteropods for example, represent up to 30% of total zooplankton species around the Prince Edward Islands (PEI; Fig. 9; Hunt et al., 2008), if these stocks deplete under future OA levels, the many other animals that rely on pteropods as a source of food will also be detrimentally impacted.

9 Conclusion

Ocean acidification is a global issue which is likely to impact the entire marine ecosystem - from plankton at the base of the food chain to fish at the top. Of particular concern is the decreasing concentration of CO_3^{2-} ions, which lowers the saturation states of $CaCO_3$ minerals (Ω_{Ar} and Ω_{Ca}) and results in detrimental seawater conditions for marine calcifiers (e.g. pteropods and corals; Aze et al., 2014; Fabry et al., 2008). Predicting when critical Ω_{Ar} threshold values will be reached is crucial for projecting the future health of marine ecosystems and for marine resources planning and management. Here we have assessed how seasonality in oceanic CO_2 will influence the future onset of Ω_{Ar} under-saturation.~~ The impacts of ocean acidification will be first felt at the seasonal scale, however our present constraint on~~ ~~Ω_{Ar} seasonality is poor due to current model and data limitations. This~~

~~represents a critical gap in our ability to accurately diagnose the influence of seasonality on the future onset and duration of critical Ω_{Ar} levels.~~

~~To overcome this issue, we first exploited new monthly global C_T and A_T climatologies to diagnose monthly Ω_{Ar} distributions for the nominal year of 2000. We then applied an independent testing approach which revealed global uncertainties in our Ω_{Ar} predictions to be ±0.14, with no strong global or seasonal biases. Finally, we combined our observational baselines with decadal trends from an ensemble of ESM under different emissions scenarios (RCPs 2.6, 4.5 and 8.5) to project our Ω_{Ar} distributions through to 2100. These results have provided new insights into the role of seasonality in setting future aragonite values and time of under-saturation onset in the global ocean.~~

The influence of seasonality was evaluated by comparing the difference in future month-long and annual-mean Ω_{Ar} under-saturation onset. Our results suggest seasonality brings forward the initial onset of month-long under-saturation by 17±10 years compared to annual mean estimates under RCP8.5, with differences extending up to 35±17 years in the North Pacific due to strong regional seasonality.

Our results also show large-scale under-saturation once atmospheric CO_2 reaches ~~486~~ 496ppm in the North Pacific, ~~506~~ 517ppm in the North Atlantic and 511ppm in the Southern Ocean, independent of emission scenario. It's important to note that seasonality in these regions was also found to be the dominate mode of variability, accounting for 84±5% of total model-based variability in the Southern Ocean (South of 30°S) and North Pacific (30°N to 70°N). This suggests IAV will not significantly alter onset times found in this study.

Under lower emission scenarios, the average time difference between month-long and annual-mean aragonite under-saturation onset increased from 14 years under RCP8.5 to 32 years under RCP4.5 in the Southern Ocean. This larger time difference under a lower emissions scenario emphasizes the importance of accounting for seasonality when projecting future OA levels under a slower emissions scenario. The spatial extent of Ω_{Ar} under-saturation is also drastically reduced under a lower emission scenario. Under RCP2.6 for example, our results show a 92.6% (or 83.6×10^6 km^2) reduction in open-ocean expose to Ω_{Ar} under-saturation compared to projections under RCP8.5, emphasising the importance of mitigating CO_2 emissions.

Seasonality also presents significant implications for the ~~influences the~~ spatial pattern of future Ω_{Ar} under-saturation.~~,~~ Here we found ~~expanding the latitudinal extent~~ month-long under-saturation extended equatorward by a global average of 3.5° (or 23×10^6 km^2) compared to annual-mean projections under RCP8.5. From a biogeochemical perspective, this is particularly concerning given ~~that~~ the regions of expansion from the poles (~40° to 50° South and North) ~~is~~ are known ~~to be a~~ as important hot-spots for $CaCO_3$ export (Sarmiento and Gruber, 2006).

Finally, the implication of our results are not limited to the higher latitudes, strong Ω_{Ar} seasonality in some subtropical regions (30°S-30°N; see Fig. 4) will likely bring forward the onset of lower Ω_{Ar} waters by similar temporal periods. Since these regions are rich with sensitive calcifying coral reef ecosystems, considering the influence of seasonality is important when estimating future OA levels and their impacts in these regions.

Acknowledgements

T.P. Sasse would like to acknowledge the funding support from the CSIRO carbon cluster. A. Lenton and R.J. Matear would like to acknowledge the funding support of CSIRO Oceans and Atmosphere and the Australian Climate Change Science Program.

References

Archer, D., Kheshgi, H., Maier, and Reimer, E. (1997), Multiple timescales for neutralization of fossil fuel CO_2, Geophys. Res. Lett., 24, 405-408, DOI: 10.1029/97gl00168

Aumont, O., and Bopp, L. (2006), Globalizing results from ocean in situ iron fertilization studies, Global Biogeochemical Cycles, 20, GB2017, DOI: 10.1029/2005gb002591

Secretariat of the Convention on Biological Diversity (2014), An Updated Synthesis of the Impacts of Ocean Acidification on Marine Biodiversity, (Eds: Hennige, S., Roberts, J. M., and Williamson, P.), Montreal, Technical Series no. 75, 99 pp.

Bednarsek, N., Tarling, G. A., Bakker, D. C. E., Fielding, S., Jones, E. M., Venables, H. J., Ward, P., Kuzirian, A., Leze, B., Feely, R. A., and Murphy, E. J. (2012), Extensive dissolution of live pteropods in the Southern Ocean, Nature Geosci, 5, 881-885, DOI: 10.1038/ngeo1635

Berner, R. A., and Honjo, S. (1981), Pelagic Sedimentation of Aragonite: Its Geochemical Significance, Science, 211, 940-942, DOI: 10.1126/science.211.4485.940

Bopp, L., Resplandy, L., Orr, J. C., Doney, S. C., Dunne, J. P., Gehlen, M., Halloran, P., Heinze, C., Ilyina, T., Séférian, R., Tjiputra, J., and Vichi, M. (2013), Multiple stressors of ocean ecosystems in the 21st century: projections with CMIP5 models, Biogeosciences, 10, 6225-6245, DOI: 10.5194/bg-10-6225-2013

Caldeira, K., and Wickett, M. E. (2003), Oceanography: Anthropogenic carbon and ocean pH, Nature, 425, 365-365, DOI: 10.1038/425365a

Caldeira, K., and Wickett, M. E. (2005), Ocean model predictions of chemistry changes from carbon dioxide emissions to the atmosphere and ocean, Journal of Geophysical Research: Oceans, 110, C09S04, DOI: 10.1029/2004JC002671

Cao, L., Caldeira, K., and Jain, A. K. (2007), Effects of carbon dioxide and climate change on ocean acidification and carbonate mineral saturation, Geophys. Res. Lett., 34, L05607, DOI: 10.1029/2006gl028605

Chan, N. C. S., and Connolly, S. R. (2013), Sensitivity of coral calcification to ocean acidification: a meta-analysis, Global Change Biology, 19, 282-290, DOI: 10.1111/gcb.12011

Dickson, A. G., and Millero, F. J. (1987), A comparison of the equilibrium constants for the dissociation of carbonic acid in seawater media, Deep Sea Research Part A. Oceanographic Research Papers, 34, 1733-1743, DOI: 10.1016/0198-0149(87)90021-5

Dickson, A. G. (1990a), Thermodynamics of the dissociation of boric acid in synthetic seawater from 273.15 to 318.15 K, Deep Sea Research Part A. Oceanographic Research Papers, 37, 755-766, DOI: 10.1016/0198-0149(90)90004-F

Dickson, A. G. (1990b), Standard potential of the reaction: AgCl(s) + 1/2H_2(g) = Ag(s) + HCl(aq), and and the standard acidity constant of the ion HSO_4^- in synthetic sea water from 273.15 to 318.15 K, The Journal of Chemical Thermodynamics, 22, 113-127, DOI: 10.1016/0021-9614(90)90074-Z

Dickson, A. G., Sabine, C. L., and Christian, J. R. (Eds.) (2007), Guide to best practices for ocean CO_2 measurements, PICES Special Publication 3, 191 pp.

Dunne, J. P., John, J. G., Shevliakova, E., Stouffer, R. J., Krasting, J. P., Malyshev, S. L., Milly, P. C. D., Sentman, L. T., Adcroft, A. J., Cooke, W., Dunne, K. A., Griffies, S. M., Hallberg, R. W., Harrison, M. J., Levy, H., Wittenberg, A. T., Phillips, P. J., and Zadeh, N. (2013), GFDL's ESM2 Global Coupled Climate–Carbon Earth System Models. Part II: Carbon System Formulation and Baseline Simulation Characteristics*, Journal of Climate, 26, 2247-2267, DOI: 10.1175/JCLI-D-12-00150.1

Durack, P. J., and Wijffels, S. E. (2010), Fifty-Year Trends in Global Ocean Salinities and Their Relationship to Broad-Scale Warming, Journal of Climate, 23, 4342-4362, DOI: 10.1175/2010jcli3377.1

Fabry, V. J., Seibel, B. A., Feely, R. A., and Orr, J. C. (2008), Impacts of ocean acidification on marine fauna and ecosystem processes, ICES Journal of Marine Science / Journal du Conseil, 65, 414-432, DOI: 10.1093/icesjms/fsn048

Garcia, H. E., Locarnini, R. A., Boyer, T. P., Antonov, J. I., Baranova, O. K., Zweng, M. M., Reagan, J. R., and Johnson, D. R. (2014a), World Ocean Atlas 2013, Volume 3: Dissolved Oxygen, Apparent Oxygen Utilization, and Oxygen Saturation, in, edited by: Levitus, S., and Mishonov, A., NOAA Atlas NESDIS 75, 27 pp.

Garcia, H. E., Locarnini, R. A., Boyer, T. P., Antonov, J. I., Baranova, O. K., Zweng, M. M., Reagan, J. R., and Johnson, D. R. (2014b), World Ocean Atlas 2013, Volume 4: Dissolved Inorganic Nutrients (phosphate, nitrate, silicate), in, edited by: Levitus, S., and Mishonov, A., NOAA Atlas NESDIS 76, 25, 25 pp.

Gruber, N., Hauri, C., Lachkar, Z., Loher, D., Frölicher, T. L., and Plattner, G.-K. (2012), Rapid Progression of Ocean Acidification in the California Current System, Science, 337, 220-223, DOI: 10.1126/science.1216773

Hunt, B. P. V., Pakhomov, E. A., Hosie, G. W., Siegel, V., Ward, P., and Bernard, K. (2008), Pteropods in Southern Ocean ecosystems, Progress In Oceanography, 78, 193-221, DOI: 10.1016/j.pocean.2008.06.001

Ilyina, T., Six, K. D., Segschneider, J., Maier-Reimer, E., Li, H., and Núñez-Riboni, I. (2013), Global ocean biogeochemistry model HAMOCC: Model architecture and performance as component of the MPI-Earth system model in different CMIP5 experimental realizations, Journal of Advances in Modeling Earth Systems, 5, 287-315, DOI: 10.1029/2012MS000178

Ishii, M., Feely, R. A., Rodgers, K. B., Park, G. H., Wanninkhof, R., Sasano, D., Sugimoto, H., Cosca, C. E., Nakaoka, S., Telszewski, M., Nojiri, Y., Mikaloff Fletcher, S. E., Niwa, Y., Patra, P. K., Valsala, V., Nakano, H., Lima, I., Doney, S. C., Buitenhuis, E. T., Aumont, O., Dunne, J. P., Lenton, A., and Takahashi, T. (2014), Air–sea CO_2 flux in the Pacific Ocean for the period 1990-2009, Biogeosciences, 11, 709-734, DOI: 10.5194/bg-11-709-2014

Karnovsky, N. J., Hobson, K. A., Iverson, S., and Hunt, G. L. J. (2008), Seasonal changes in diets of seabirds in the North Water Polynya: a multiple-indicator approach, Marine Ecology Progress Series, 357, 291-299, DOI: 10.3354/meps07295

Kleypas, J. A., Buddemeier, R. W., Archer, D., Gattuso, J.-P., Langdon, C., and Opdyke, B. N. (1999), Geochemical consequences of increased atmospheric carbon dioxide on coral reefs, Science, 284, 118-120, DOI: 10.1126/science.284.5411.118

Le Quéré, C., Rödenbeck, C., Buitenhuis, E. T., Conway, T. J., Langenfelds, R., Gomez, A., Labuschagne, C., Ramonet, M., Nakazawa, T., Metzl, N., Gillett, N., and Heimann, M. (2007), Saturation of the Southern Ocean CO_2 Sink Due to Recent Climate Change, Science, 316, 1735-1738, DOI: 10.1126/science.1136188

Le Quéré, C., Moriarty, R., Andrew, R. M., Peters, G. P., Ciais, P., Friedlingstein, P., Jones, S. D., Sitch, S., Tans, P., Arneth, A., Boden, T. A., Bopp, L., Bozec, Y., Canadell, J. G., Chini, L. P., Chevallier, F., Cosca, C. E., Harris, I., Hoppema, M., Houghton, R. A., House, J. I., Jain, A. K., Johannessen, T., Kato, E., Keeling, R. F., Kitidis, V., Klein Goldewijk, K., Koven, C., Landa, C. S., Landschützer, P., Lenton, A., Lima, I. D., Marland, G., Mathis, J. T., Metzl, N., Nojiri, Y., Olsen, A., Ono, T., Peng, S., Peters, W., Pfeil, B., Poulter, B., Raupach, M. R., Regnier, P., Rödenbeck, C., Saito, S., Salisbury, J. E., Schuster, U., Schwinger, J., Séférian, R., Segschneider, J., Steinhoff, T., Stocker, B. D., Sutton, A. J., Takahashi, T., Tilbrook, B., van der Werf, G. R., Viovy, N., Wang, Y. P., Wanninkhof, R., Wiltshire, A., and Zeng, N. (2015), Global carbon budget 2014, Earth Syst. Sci. Data, 7, 47-85, DOI: 10.5194/essd-7-47-2015

Lenton, A., Codron, F., Bopp, L., Metzl, N., Cadule, P., Tagliabue, A., and Le Sommer, J. (2009), Stratospheric ozone depletion reduces ocean carbon uptake and enhances ocean acidification, Geophys. Res. Lett., 36, L12606, DOI: 10.1029/2009gl038227

Lenton, A., Metzl, N., Takahashi, T., Kuchinke, M., Matear, R. J., Roy, T., Sutherland, S. C., Sweeney, C., and Tilbrook, B. (2012), The observed evolution of oceanic pCO_2 and its drivers over the last two decades, Global Biogeochem. Cycles, 26, GB2021, DOI: 10.1029/2011gb004095

Lenton, A., Tilbrook, B., Law, R. M., Bakker, D., Doney, S. C., Gruber, N., Ishii, M., Hoppema, M., Lovenduski, N. S., Matear, R. J., McNeil, B. I., Metzl, N., Mikaloff Fletcher, S. E., Monteiro, P. M. S., Rödenbeck, C., Sweeney, C., and Takahashi, T. (2013), Sea–air CO_2 fluxes in the Southern Ocean for the period 1990-2009, Biogeosciences, 10, 4037-4054, DOI: 10.5194/bg-10-4037-2013

Levitus, S., Antonov, J., and Boyer, T. (2005), Warming of the world ocean, 1955-2003, Geophys. Res. Lett., 32, L02604, DOI: 10.1029/2004gl021592

Locarnini, R. A., Mishonov, A. V., Antonov, J. I., Boyer, T. P., Garcia, H. E., Baranova, O. K., Zweng, M. M., Paver, C. R., Reagan, J. R., Johnson, D. R., Hamilton, M., and Seidov, D. (2013), World Ocean Atlas 2013, Volume 1: Temperature, in, edited by: S. Levitus, E., and A. Mishonov, T. E., NOAA Atlas NESDIS 73, 40 pp.

Lyman, J. M., Good, S. A., Gouretski, V. V., Ishii, M., Johnson, G. C., Palmer, M. D., Smith, D. M., and Willis, J. K. (2010), Robust warming of the global upper ocean, Nature, 465, 334-337, DOI: 10.1038/nature09043

Mathis, J. T., and Questel, J. M. (2013), Assessing seasonal changes in carbonate parameters across small spatial gradients in the Northeastern Chukchi Sea, Continental Shelf Research, 67, 42-51, DOI: 10.1016/j.csr.2013.04.041

McNeil, B. I., and Matear, R. J. (2008), Southern Ocean acidification: A tipping point at 450-ppm atmospheric CO_2, Proceedings of the National Academy of Sciences, 105, 18860-18864, DOI: 10.1073/pnas.0806318105

McNeil, B. I., Tagliabue, A., and Sweeney, C. (2010), A multi-decadal delay in the onset of corrosive 'acidified' waters in the Ross Sea of Antarctica due to strong air-sea CO_2 disequilibrium, Geophys. Res. Lett., 37, L19607, DOI: 10.1029/2010gl044597

McNeil, B. I., and Matear, R. J. (2013), The non-steady state oceanic CO_2 signal: its importance, magnitude and a novel way to detect it, Biogeosciences, 10, 2219-2228, DOI: 10.5194/bg-10-2219-2013

Mehrbach, C., Culberson, C. H., Hawley, J. E., and Pytkowicz, R. M. (1973), Measurement of the Apparent Dissociation Constants of Carbonic Acid in Seawater at Atmospheric Pressure, Limnology and Oceanography, 18, 897-907

Meinshausen, M., Smith, S. J., Calvin, K., Daniel, J. S., Kainuma, M. L. T., Lamarque, J. F., Matsumoto, K., Montzka, S. A., Raper, S. C. B., Riahi, K., Thomson, A., Velders, G. J. M., and Vuuren, D. P. P. (2011), The RCP greenhouse gas concentrations and their extensions from 1765 to 2300, Climatic Change, 109, 213-241, DOI: 10.1007/s10584-011-0156-z

Monteiro, P., Schuster, U., Hood, M., Lenton, A., Metzl, N., Olsen, A., Rogers, K., Sabine, C., Takahashi, T., Tilbrook, B., Yoder, J., Wanninkhof, R., and Watson, A. J.: A Global Sea Surface Carbon Observing System: Assessment of Changing Sea Surface CO_2 and Air-Sea CO_2 Fluxes, Proceedings of OceanObs'09: Sustained Ocean Observations and Information for Society (Vol. 2), Venice, Italy, 21-25 September 2009, 2010.

Mucci, A. (1983), The solubility of calcite and aragonite in seawater at various salinities, temperatures, and one atmosphere total pressure, American Journal of Science, 283, 780-799, DOI: 10.2475/ajs.283.7.780

Newton, J. A., Feely, R. A., Jewett, E. B., Williamson, P., and Mathis, J. (2014), Global Ocean Acidification Observing Network: Requirements and Governance Plan, First ed., 60 pp.

Orr, J. C., Fabry, V. J., Aumont, O., Bopp, L., Doney, S. C., Feely, R. A., Gnanadesikan, A., Gruber, N., Ishida, A., Joos, F., Key, R. M., Lindsay, K., Maier-Reimer, E., Matear, R., Monfray, P., Mouchet, A., Najjar, R. G., Plattner, G.-K., Rodgers, K. B., Sabine, C. L., Sarmiento, J. L., Schlitzer, R., Slater, R. D., Totterdell, I. J., Weirig, M.-F., Yamanaka, Y., and Yool, A. (2005), Anthropogenic ocean acidification over the twenty-first century and its impact on calcifying organisms, Nature, 437, 681-686, DOI: 10.1038/nature04095

Palmer, J. R., and Totterdell, I. J. (2001), Production and export in a global ocean ecosystem model, Deep Sea Research Part I: Oceanographic Research Papers, 48, 1169-1198, DOI: 10.1016/S0967-0637(00)00080-7

Pilcher, D. J., Brody, S. R., Johnson, L., and Bronselaer, B. (2015), Assessing the abilities of CMIP5 models to represent the seasonal cycle of surface ocean pCO_2, Journal of Geophysical Research: Oceans, 120, 4625-4637, DOI: 10.1002/2015JC010759

Popova, E. E., Yool, A., Aksenov, Y., Coward, A. C., and Anderson, T. R. (2014), Regional variability of acidification in the Arctic: a sea of contrasts, Biogeosciences, 11, 293-308, DOI: 10.5194/bg-11-293-2014

Ricke, K. L., Orr, J. C., Schneider, K., and Caldeira, K. (2013), Risks to coral reefs from ocean carbonate chemistry changes in recent earth system model projections, Environmental Research Letters, 8, 034003, DOI: 10.1088/1748-9326/8/3/034003

Riley, J. P., and Tongudai, M. (1967), The major cation/chlorinity ratios in sea water, Chemical Geology, 2, 263-269, DOI: 10.1016/0009-2541(67)90026-5

Sarma, V. V. S. S., Lenton, A., Law, R. M., Metzl, N., Patra, P. K., Doney, S., Lima, I. D., Dlugokencky, E., Ramonet, M., and Valsala, V. (2013), Sea–air CO_2 fluxes in the Indian Ocean between 1990 and 2009, Biogeosciences, 10, 7035-7052, DOI: 10.5194/bg-10-7035-2013

Sarmiento, J. L., and Gruber, N. (2002), Sinks for Anthropogenic Carbon, Physics Today, 55, 30-36, DOI: 10.1063/1.1510279

Sarmiento, J. L., and Gruber, N. (2006), Ocean biogeochemical dynamics, Princeton University Press, 526 pp.

Sasse, T. P., McNeil, B. I., and Abramowitz, G. (2013a), A new constraint on global air-sea CO2 fluxes using bottle carbon data, Geophysical Research Letters, 40, 1594-1599, DOI: 10.1002/grl.50342

Sasse, T. P., McNeil, B. I., and Abramowitz, G. (2013b), A novel method for diagnosing seasonal to inter-annual surface ocean carbon dynamics from bottle data using neural networks, Biogeosciences, 10, 4319-4340, DOI: 10.5194/bg-10-4319-2013

Schuster, U., Watson, A. J., Bates, N. R., Corbiere, A., Gonzalez-Davila, M., Metzl, N., Pierrot, D., and Santana-Casiano, M. (2009), Trends in North Atlantic sea-surface fCO_2 from 1990 to 2006, Deep Sea Research Part II: Topical Studies in Oceanography, 56, 620-629, DOI: 10.1016/j.dsr2.2008.12.011

Séférian, R., Bopp, L., Gehlen, M., Orr, J., Ethé, C., Cadule, P., Aumont, O., Salas y Mélia, D., Voldoire, A., and Madec, G. (2013), Skill assessment of three earth system models with common marine biogeochemistry, Climate Dynamics, 40, 2549-2573, DOI: 10.1007/s00382-012-1362-8

Shaw, E. C., Munday, P. L., and McNeil, B. I. (2013), The role of CO2 variability and exposure time for biological impacts of ocean acidification, Geophysical Research Letters, 40, 4685-4688, DOI: 10.1002/grl.50883

Steinacher, M., Joos, F., Frölicher, T. L., Plattner, G. K., and Doney, S. C. (2009), Imminent ocean acidification in the Arctic projected with the NCAR global coupled carbon cycle-climate model, Biogeosciences, 6, 515-533, DOI: 10.5194/bg-6-515-2009

Takahashi, T., Sutherland, S. C., Wanninkhof, R., Sweeney, C., Feely, R. A., Chipman, D. W., Hales, B., Friederich, G., Chavez, F., Sabine, C. L., Watson, A., Bakker, D. C. E., Schuster, U., Metzl, N., Yoshikawa-Inoue, H., Ishii, M., Midorikawa, T., Nojiri, Y., Körtzinger, A., Steinhoff, T., Hoppema, M., Olafsson, J., Arnarson, T. S., Tilbrook, B., Johannessen, T., Olsen, A., Bellerby, R. G. J., Wong, C. S., Delille, B., Bates, N. R., and de Baar, H. J. W. (2009), Climatological mean and decadal change in surface ocean pCO_2, and net sea-air CO_2 flux over the global oceans, Deep Sea Research Part II: Topical Studies in Oceanography, 56, 554-577, DOI: 10.1016/j.dsr2.2008.12.009

Takahashi, T., Sutherland, S. C., Chipman, D. W., Goddard, J. G., Ho, C., Newberger, T., Sweeney, C., and Munro, D. R. (2014), Climatological distributions of pH, pCO_2, total CO_2, alkalinity, and $CaCO_3$ saturation in the global surface ocean, and temporal changes at selected locations, Marine Chemistry, 164, 95-125, DOI: 10.1016/j.marchem.2014.06.004

Tjiputra, J. F., Olsen, A., Bopp, L., Lenton, A., Pfeil, B., Roy, T., Segschneider, J., Totterdell, I., and Heinze, C. (2014), Long-term surface pCO_2 trends from observations and models, Tellus B, DOI: 10.3402/tellusb.v66.23083

Tupper, M., Tan, M. K., Tan, S. L., Radius, M. J., and Abdullah, S. (2011), ReefBase: a global information system on coral reefs, http://www.reefbase.org, Zahariev, K., Christian, J. R., and Denman, K. L. (2008), Preindustrial, historical, and fertilization simulations using a global ocean carbon model with new parameterizations of iron limitation, calcification, and N2 fixation, Progress in Oceanography, 77, 56-82, DOI: 10.1016/j.pocean.2008.01.007

Zweng, M. M., Reagan, J. R., Antonov, J. I., Locarnini, R. A., Mishonov, A. V., Boyer, T. P., Garcia, H. E., Baranova, O. K., Johnson, D. R., D.Seidov, and Biddle, M. M. (2013), World Ocean Atlas 2013, Volume 2: Salinity, in, edited by: Levitus, S., and Mishonov, A., NOAA Atlas NESDIS 74, 39 pp.

Region	Zone[a]	RSE[b]	*N*[c]
Arctic Ocean	1	0.22	673
Sup-Polar North Atlantic	2	0.13	2380
Sub-Tropical North Atlantic	3	0.11	1205
Equatorial Atlantic	4	0.16	565
Sub-Tropical South Atlantic	5	0.12	527
Sub-Polar North Pacific	6	0.18	1541
Sub-Tropical North Pacific	7	0.15	1412
Equatorial Pacific	8	0.16	764
Sub-Tropical South Pacific	9	0.15	1353
Sub-Tropical North Indian	10	0.13	137
Equatorial Indian	11	0.13	481
Sub-Tropical South Indian	12	0.11	1340
Southern Ocean	13	0.10	2923
Subantarctic waters	14	0.11	1426
Global		**0.138**	**16727**

Table 1: Regional and global skill evaluation for predicting Ω_{Ar} (see Fig. S3 for map of spatial division).

[a] Corresponding geographical region in Fig. S3

[b] Residual Standard Error

[c] number of measurements

Model	Ocean Resolution	BGC model	Reference
CanESM2	0.9-1.4°	CMOC	Zahariev et al. (2008)
GFDL-ESM2G	0.3-1°	TOPAZ2	Dunne et al (2013)
HadGEM2-ES	0.3-1°	Diat-HadOCC	Palmer and Totterdell (2001)
IPSL-CM5A-LR	0.5-2°	PISCES	Aumont and Bopp (2006), Séférian et al. (2013)
IPSL-CM5A-MR	0.5-2°	PISCES	Aumont and Bopp (2006), Séférian et al. (2013)
MPI-ESM-MR	0.4°	HAMOCC5.2	Ilyina et al. (2013)

Table 2: Main characteristics of the 6 ESM used in this study.

RCP	Month-long onset mean±sd (RCP8.5)	Atmospheric CO_2 mean±sd (RCP8.5)	Corr. to RCP8.5	Number of 1°×1° grid cells
		North Pacific (30°N to 65°N)		
4.5	2057±24 (2040±15)	492±45 (501±61)	0.75	475
2.6	2022±21 (2022±15)	406±28 (428±46)	0.81	110
		North Atlantic (30°N to 70°N)		
4.5	2061±17 (2047±12)	505±36 (530±51)	0.86	37
2.6	2024±20 (2016±15)	415±39 (410±40)	0.88	3
		Southern Ocean (South of 45°S)		
4.5	2064±19 (2045±9)	505±30 (518±46)	0.75	2619
2.6	2033±15 (2030±8)	428±19 (450±29)	0.66	154

Table 3: Comparison between future aragonite projections under RCP4.5 and 2.6 relative to RCP8.5. (Note to editor: These values have been adjusted for coastal data exclusion)

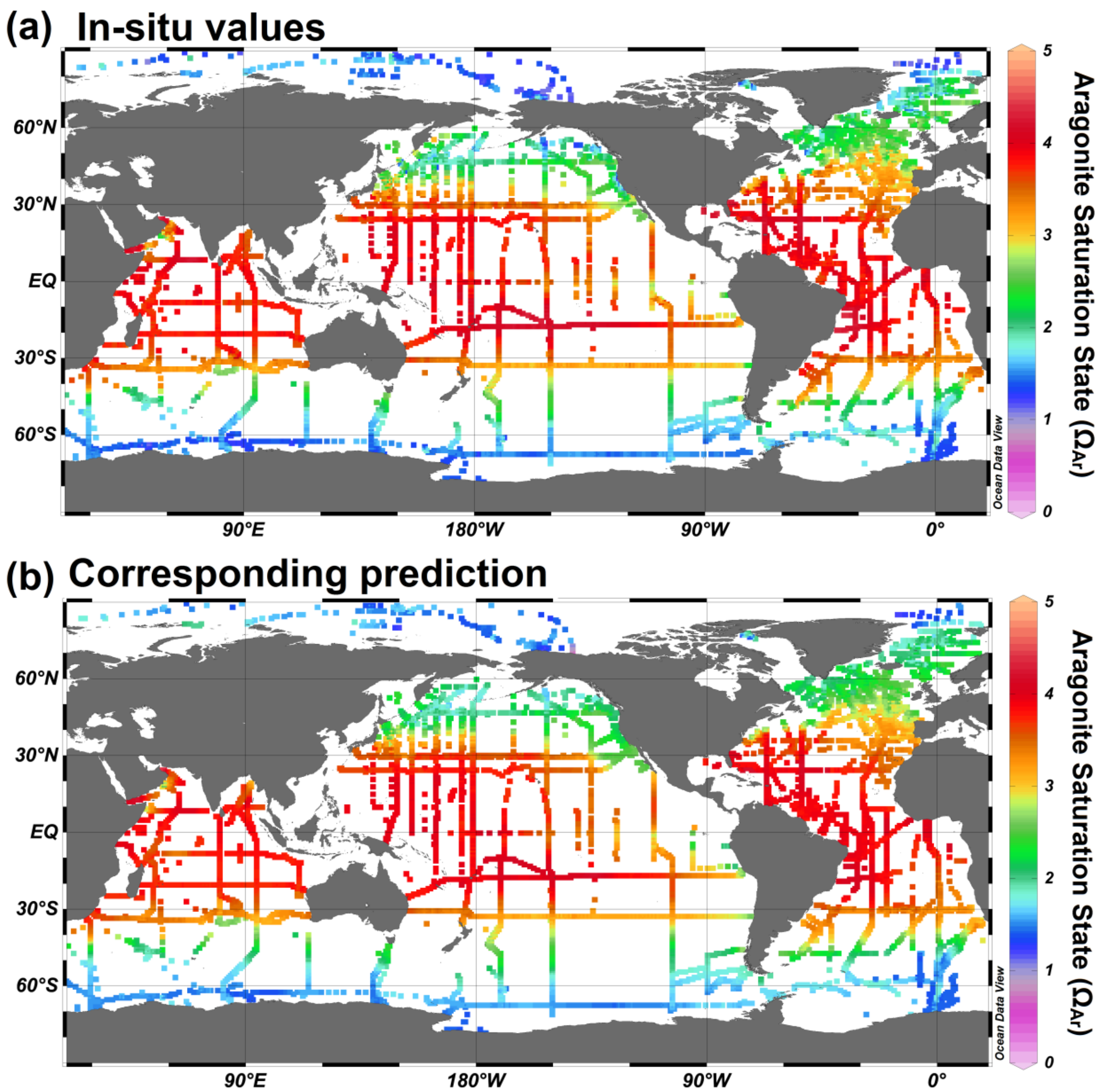

Figure 1: (a) In-situ Ω_{Ar} measurements normalised to the year 2000; (b) corresponding 1°×1° Ω_{Ar} prediction for the same month and location for the nominal year for 2000 (see ~~Supplementary A~~ Supp. Fig S1 for our monthly Ω_{Ar} distributions).

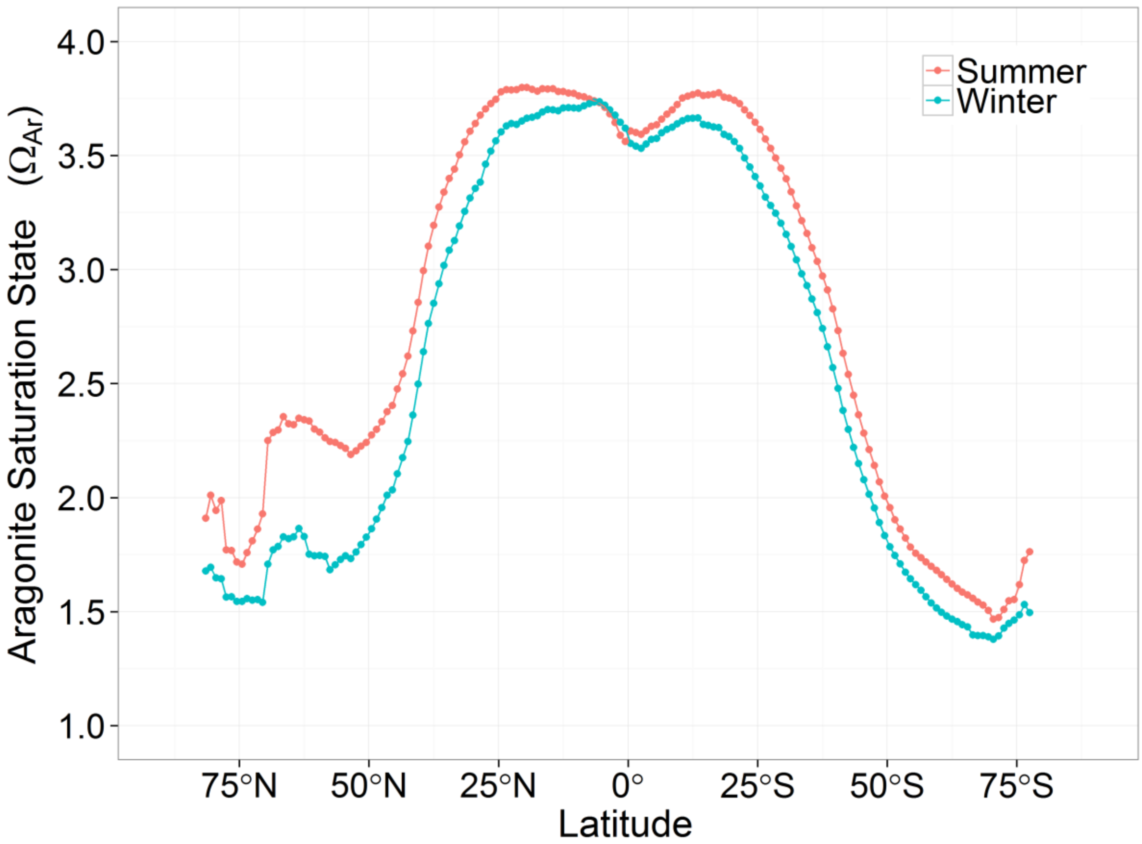

Figure 2: Zonal mean Ω_{Ar} predictions for winter and summer (joined dots). ~~In-situ Ω_{Ar} values normalized to the year 2000.~~ Summer and winter months were defined as June through to August and December through to February for Northern Hemisphere respectively, while Southern Hemisphere differed by 6 months.

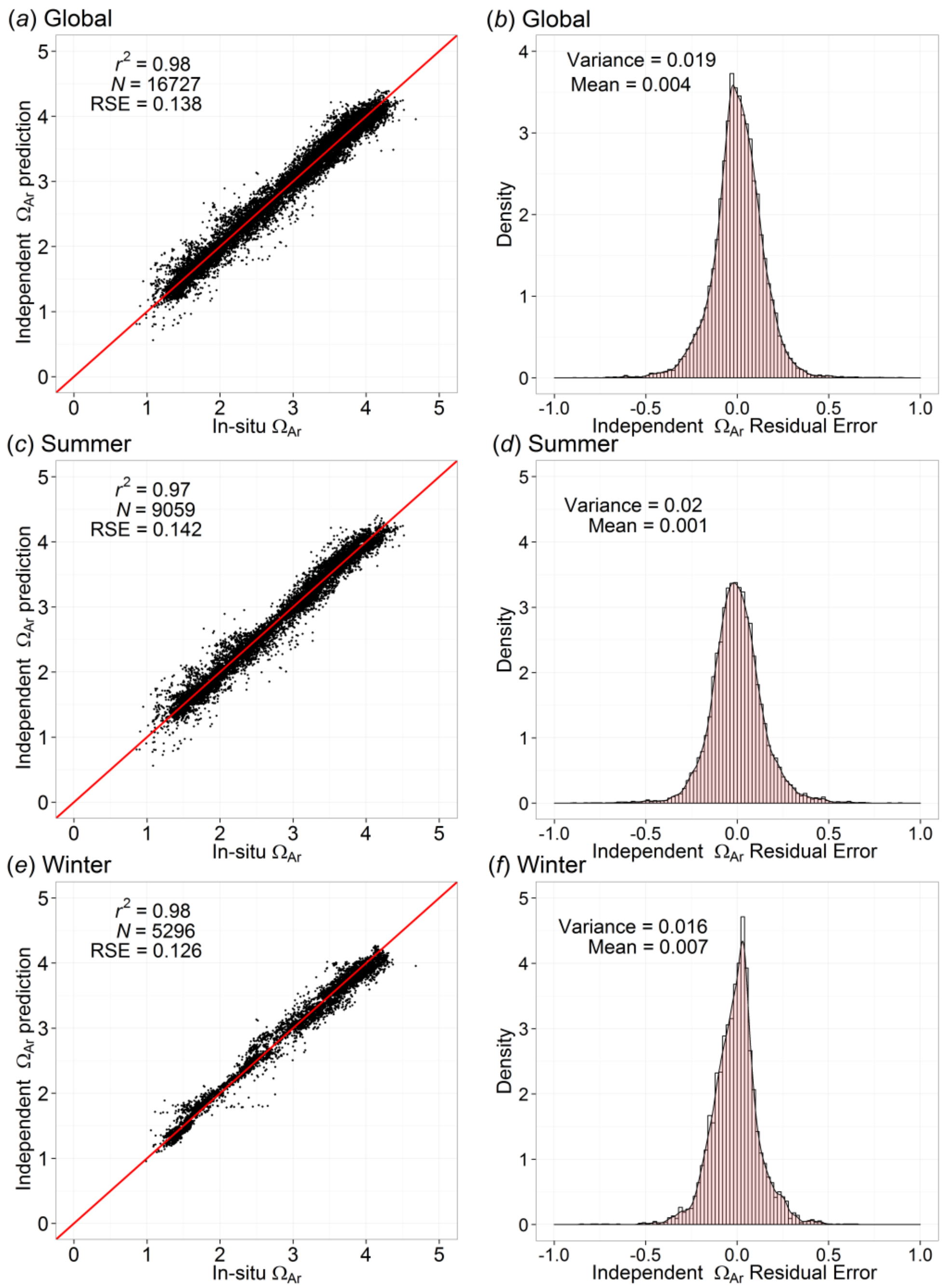

Figure 3: Statistical plots comparing global Ω_{Ar} values calculated via the network of in-situ ~~network of~~ C_T and A_T measurements~~,~~ and independently predicted C_T and A_T values ~~via the approach~~ of Sasse et al. (2013b). (a) Global independent predictions versus in-situ values, where the red line represents y = x relationship (b) Global distribution of ~~the~~ independent residual errors (c,e) Summer- and Winter-time independent predictions versus in-situ values (d,f) Summer- and Winter-time distribution of the independent residual errors. Summer and Winter months were defined as May through to September and November through to March for Northern Hemisphere respectively, while Southern Hemisphere differed by 6 months.

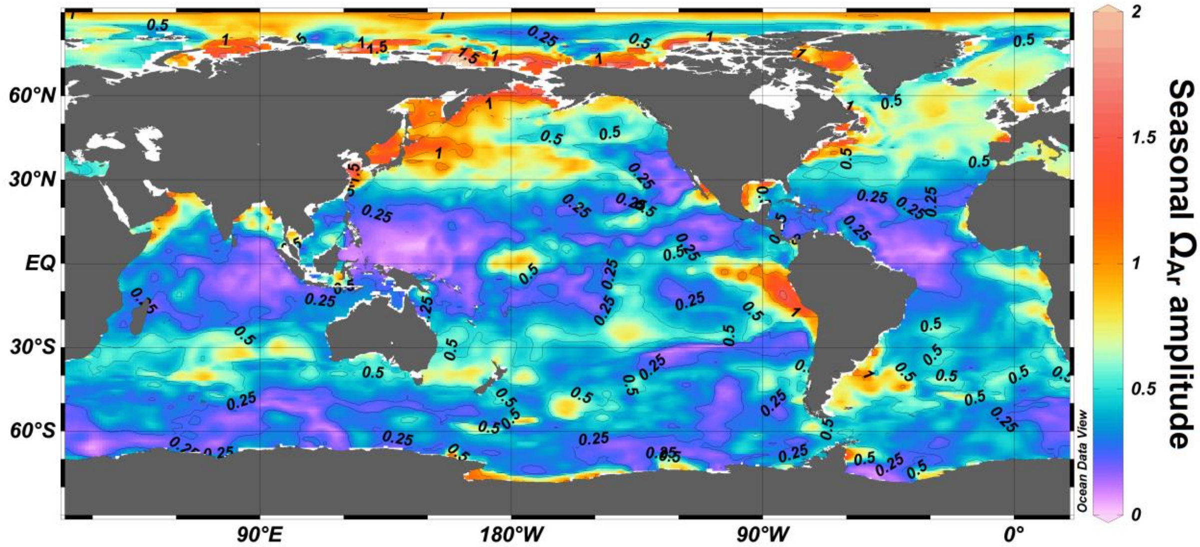

Figure 4: Seasonal Ω_{Ar} amplitudes for the nominal year of 2000. Seasonal amplitudes were calculated as the maximum minus minimum monthly Ω_{Ar} values in each 1°x1° cell (see Fig. S1 for monthly Ω_{Ar} distributions).

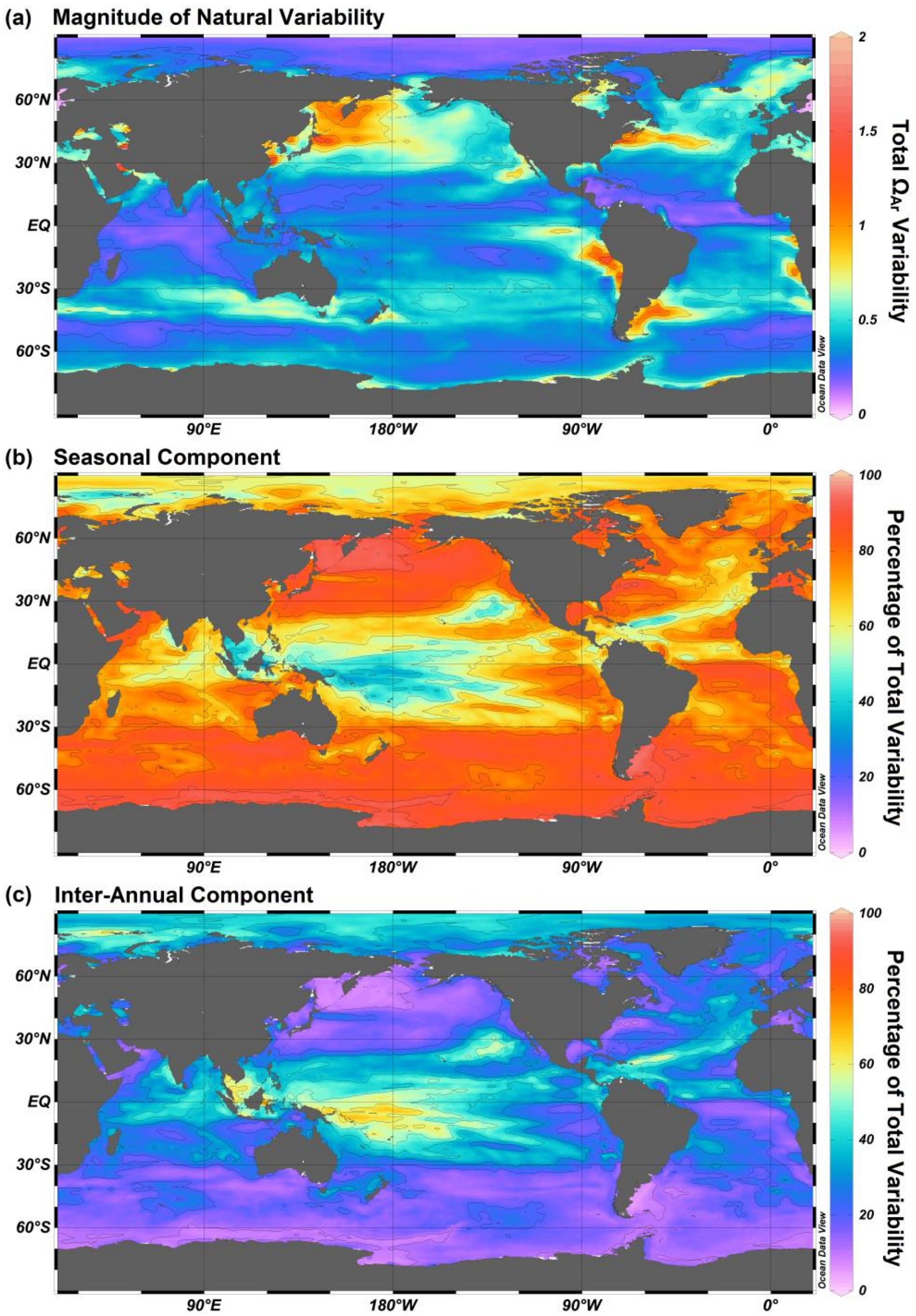

Figure 5: Model-based comparison of seasonal and inter-annual variability for ocean surface Ω_{Ar}. (a) Total magnitude of variability as estimated from the ensemble of ESM. Here seasonal variability was calculated as the mean seasonal amplitude between 2006 and 2016, while IAV was calculated via the standard-deviation in de-trended annual mean projections between 2006 and 2100; (b) Relative contribution of seasonal variability to the total variability (in percentage) (c) Relative contribution of inter-annual variability to the total variability (in percentage).

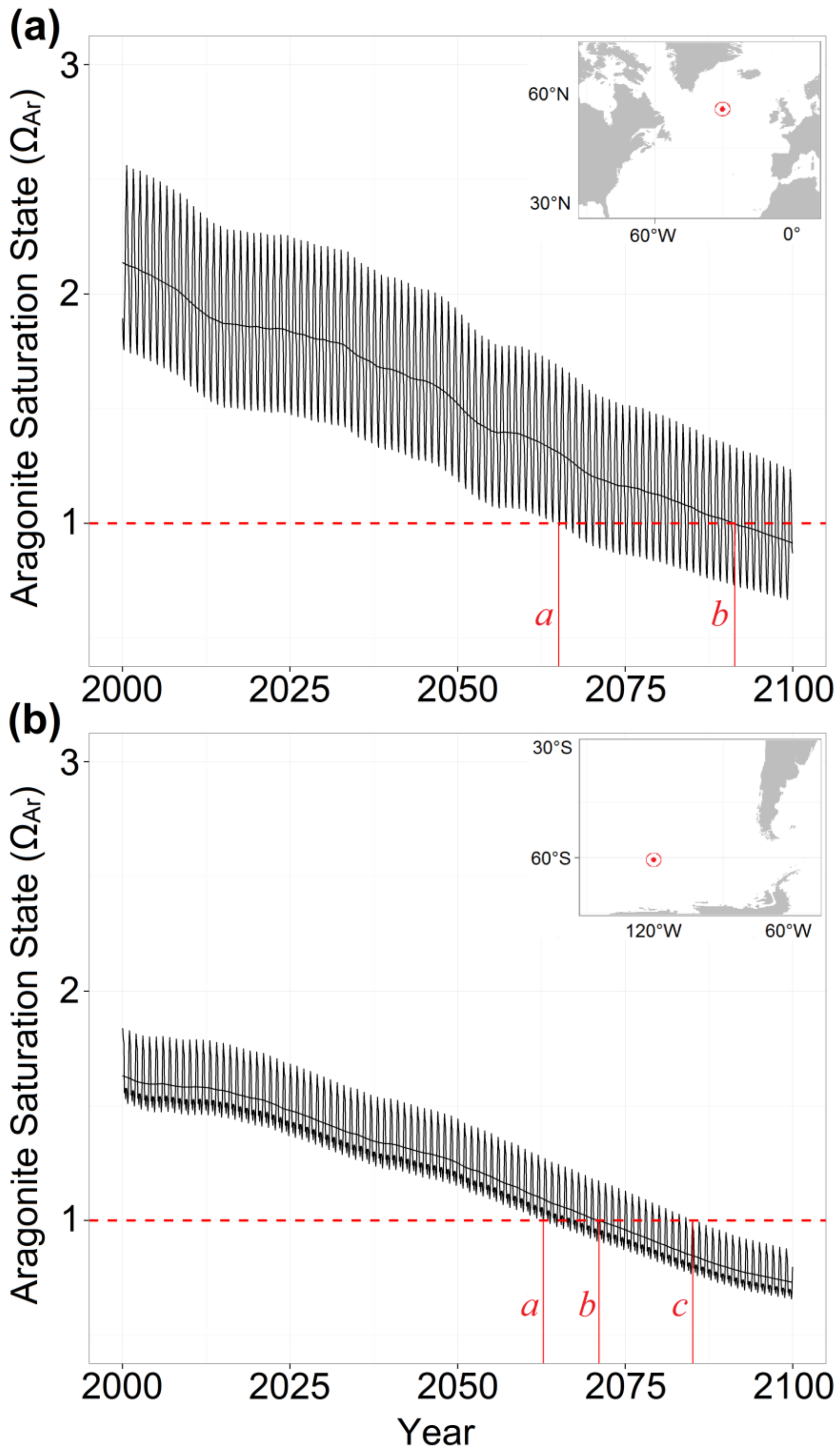

Figure 6: ~~Under RCP8.5 the f~~ Future aragonite under-saturation states (Ω_{Ar}) at locations in the (a) North Atlantic and (b) Southern Ocean under the *business-as-usual* (RCP8.5). The influence of seasonal variability accelerates under-saturation conditions by 27 and 8 years relative to annual-mean estimates (black line) in the North Atlantic and Southern Ocean, respectively. The red points *a*, *b*, and *c* denote the time when month-long, annual-mean and permanent under-saturation occurs, respectively.

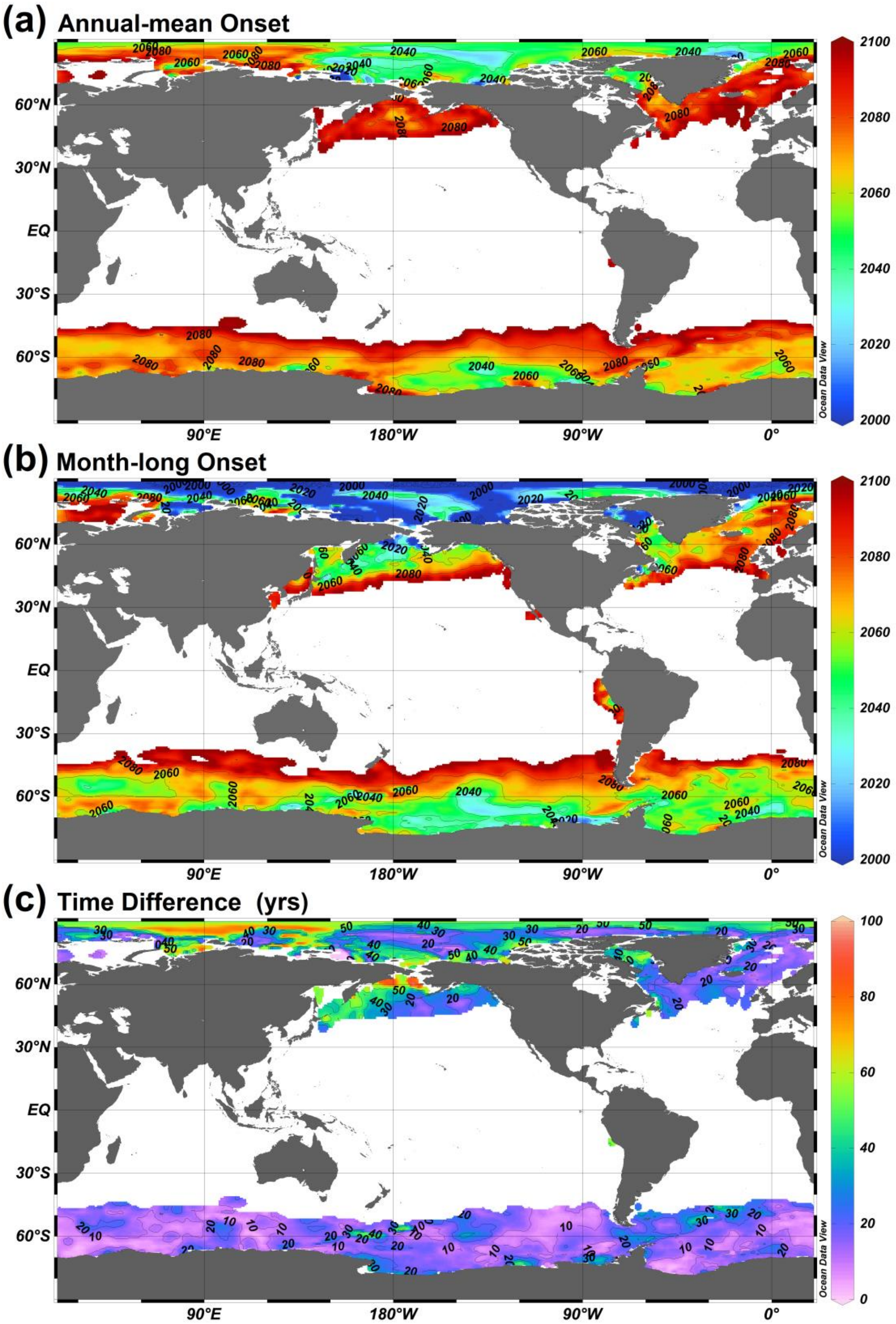

Figure 7: Estimated onset year for aragonite under-saturation under RCP8.5 for (a) annual-mean and (b) one-month. (c) Time difference (years) between annual-mean and month-long estimates.

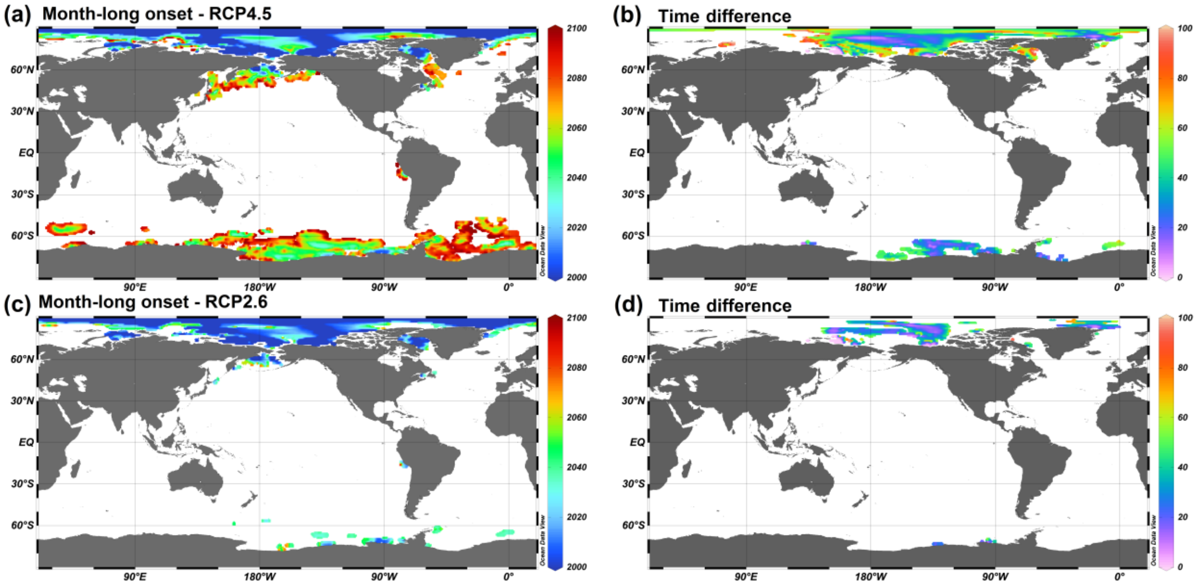

Figure 8: Onset year for month-long ocean surface aragonite under-saturation for (a) RCP4.5 and (c) RCP2.6. Time difference (years) between month-long and annual-mean surface aragonite under-saturation onset under (b) RCP4.5 and (d) RCP2.6.

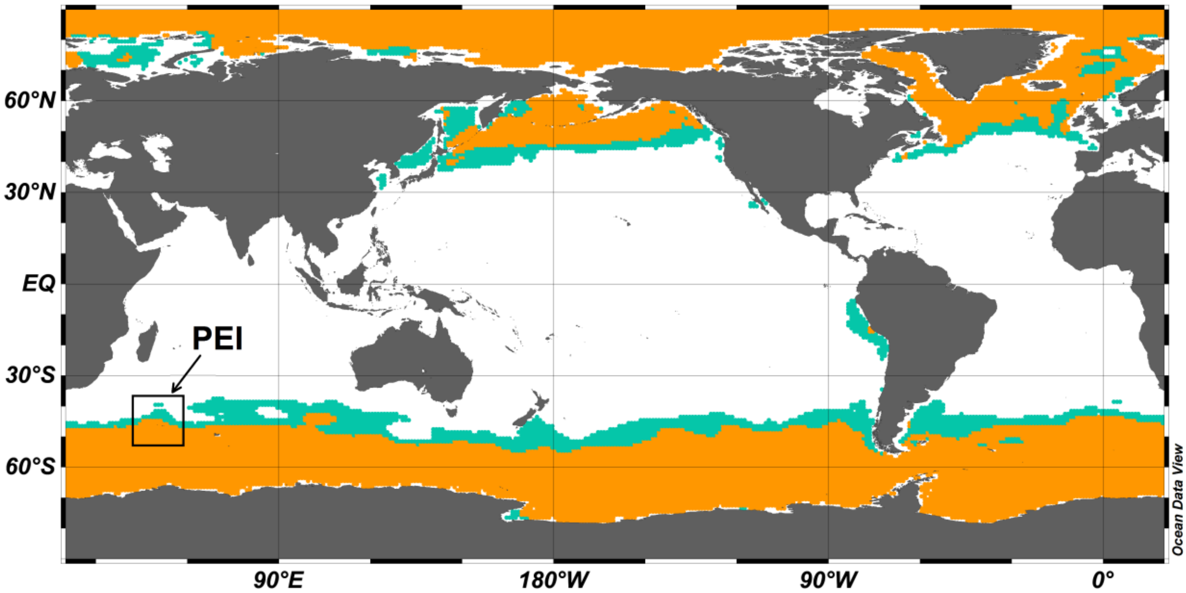

Figure 9: Surface area exposed to at least month-long (blue) and annual-mean (orange) aragonite under-saturation in the year 2100 under RCP8.5. The blue region represents $\sim 23\times10^6$ km^2. The area labelled PEI represents the pteropod study region of Hunt et al. (2008) around the Prince Edward Islands.